

Medical Sciences Division

Department of Physiology, Anatomy & Genetics

Comparison of different therapies for Neonatal Diabetes – Glibenclamide vs Insulin

Author: Michaela Iberl

University of Oxford

St Anne's College

Supervisor: Professor Frances M Ashcroft

A dissertation submitted for the degree of

Master of Science by Research (MSc Res)

Trinity 2012

Table of Contents

Abstract 1

List of Figures 3

List of Tables 5

List of Abbreviations 6

1. Introduction 8

1.1 The K_{ATP} channel in the pancreatic β-cell …… 8

1.1.1 The discovery of the pancreatic K_{ATP} channel …… 8

1.1.2 The structure of the pancreatic K_{ATP} channel …… 9

1.1.3 K_{ATP} channel regulation and insulin secretion …… 12

1.2 K_{ATP} channel mutations …… 15

1.2.1 Congenital hyperinsulinism of infancy (CHI) …… 15

1.2.2 Neonatal diabetes mellitus (ND) …… 17

1.3 Therapy for diseases caused by K_{ATP} channel mutation …… 20

1.3.1 Treatment of congenital hyperinsulinism of infancy (CHI) …… 20

1.3.2 Treatment of neonatal diabetes (ND) …… 21

1.4 The V59M mouse model …… 23

2. Methods and Materials 25

2.1 A mouse model of Neonatal Diabetes - the inducible β-V59M (iβ-V59M) mouse …… 25

2.1.1 Generation of iβ-V59M mice …… 25

2.1.2 Genotyping …… 27

2.1.3 Animal care …… 28

2.1.4 Gene induction and pellet implantation …… 28

2.1.5 Mouse body mass and blood glucose monitoring …… 30

2.1.6 Food and water intake experiments ……... 30

2.2 Glucose tolerance tests …… 31

2.3 Pancreatic islet studies …… 31

2.3.1 Isolation of pancreatic islets using enzyme digestion …….. 31

2.3.2 Insulin secretion experiments …….. 33

2.3.3 Insulin secretion experiments using static incubation …….. 34

2.4 Immunohistochemistry …….. 35

2.5 Statistical analysis …….. 37

3. Results 39

3.1 Iβ-V59M mouse model: blood glucose homeostasis and body weight …….. 39

3.1.1 Expression of the Kir6.2-V59M mutation causes diabetes ……. 39

3.1.2 Glibenclamide and insulin therapy normalize blood glucose levels ……... 42

3.1.3 Glibenclamide and insulin therapy have no effect on body weight …… 44

3.1.4 Mice bred on a pure genetic background develop a more severe phenotype …… 47

3.2 The effect of glibenclamide and insulin on glucose tolerance …… 49

3.2.1 Glucose tolerance tests reveal a gender difference in response to glucose ……... 50

3.2.2 The response of untreated and treated diabetic mice to an IPGTT …….. 52

3.2.3 The response of untreated and treated diabetic mice to an OGTT ……. 56

3.3 The effect of glibenclamide and insulin therapy on islet function and morphology …….. 60

3.3.1 Insulin secretion differs depending on therapy …… 61

3.3.2 Insulin treatment fails to preserve insulin content …… 65

3.3.3 The effect of insulin and glibenclamide therapy on pancreatic islets …… 67

3.4 Insulin secretion: in vitro static incubation …….. 74

3.4.1 Dimethyl sulfoxide (DMSO) does not decrease insulin secretion ……... 75

3.4.2 Glibenclamide initiates more insulin secretion in induced iβ-V59M mice …… 76

3.4.3 Insulin content is not altered in induced iβ-V59M mice ……... 79

3.5 The effect of glibenclamide on body weight and blood glucose in wild-type mice …….. 81

3.5.1 Glibenclamide therapy does not cause a decrease in body weight …….. 81

3.5.2 Blood glucose is increased after glibenclamide therapy …….. 83

4. Discussion 84

4.1 The iβ-V59M mouse model: expression of neonatal diabetes in adulthood …….. 84

4.1.1 The Kir6.2-V59M mutation in pancreatic β-cells causes severe diabetes …….. 84

4.1.2 The effect of diabetes on pancreatic islets …….... 85

4.1.3 Glucose tolerance is severely impaired …… 87

4.1.4 Male iß-V59M mice develop severe symptoms caused by diabetes …… 87

4.2 Insulin – diabetes treatment without affecting the K_{ATP} channel … 88

4.2.1 Insulin therapy normalizes blood glucose concentrations and does not affect body weight …… 88

4.2.2 The effect of insulin therapy on the pancreatic islet …… 89

4.2.3 Insulin therapy and glucose tolerance ……... 91

4.3 Glibenclamide – binding to the K_{ATP} channel leads to insulin secretion …….. 92

4.3.1 The effect of glibenclamide on blood glucose and body weight 92

4.3.2 Glibenclamide therapy fully preserves pancreatic islets ……. 94

4.3.3 Glibenclamide partially, but not completely, corrects glucose tolerance …… 95

4.4 Conclusion ……... 95

4.5 Future directions …… 96

References 97

Abstract

Comparison of different therapies for Neonatal Diabetes – Glibenclamide vs Insulin

Michaela Iberl, St Anne's College, University of Oxford

Submitted for the degree of MSc (Res), Trinity 2012

Gain-of-function mutations in the Kir6.2 and SUR subunits of the K_{ATP} channel are associated with neonatal diabetes (ND). I used a mouse model selectively expressing the Kir6.2-V59M mutation in pancreatic β-cells (inducible iβ-V59M) to compare the effects of sulphonylurea and insulin therapy on neonatal diabetes. Gene expression was induced in adulthood, which caused severe hyperglycaemia and resulted in a major decrease in insulin content, pancreatic β-cell area, pancreatic islet number, single islet size and total islet area. Insulin secretion and glucose tolerance were also severely impaired.

To determine if the preservation of physiological blood glucose levels (~4mM) alone is sufficient to prevent these effects, or if the closure of the K_{ATP} channel is also required, induced iβ-V59M mice were implanted with insulin pellets or a high-dose glibenclamide pellet. Insulin therapy restored blood glucose levels but failed to fully preserve pancreatic islet and β-cell morphology and function. Conversely,

glibenclamide therapy reduced elevated blood glucose concentrations down to a physiological range *and* maintained pancreatic islet and β-cell morphology and function. These findings have implications for treatment of human patients suffering from neonatal diabetes.

List of Figures

Figure 1.1: The pancreatic K_{ATP} channel ……... . 10

Figure 1.2: Membrane Topology model of SUR1 and Kir6.2 …….. 11

Figure 1.3: The role of the pancreatic K_{ATP} channel in insulin secretion …… 13

Figure 1.4: Congenital hyperinsulinism of infancy (CHI) …… 16

Figure 1.5: Neonatal diabetes (ND) …… 19

Figure 2.1: The cre ER-loxP system ……. 26

Figure 2.2: Liberase injection into the bile duct ……. 32

Figure 2.3: Insulin staining using indirect immunohistochemistry …….. 36

Figure 3.1: Free-fed blood glucose - glibenclamide treatment …… 40

Figure 3.2: Free-fed blood glucose - insulin treatment ……. 41

Figure 3.3: Body weight - glibenclamide treatment ……... . 45

Figure 3.4: Body weight - insulin treatment …… 46

Figure 3.5: IPGTT and OGTT: control vs uninduced iβ-V59M mice ……..... 51

Figure 3.6: Intraperitoneal glucose tolerance test (IPGTT) …….. 54

Figure 3.7: Oral glucose tolerance test (OGTT) …… 59

Figure 3.8: Insulin secretion: glibenclamide treated induced iβ-V59M mice ……. 63

Figure 3.9: Insulin secretion: insulin treated induced iβ-V59M mice …….. 64

Figure 3.10: Insulin content …… . 66

Figure 3.11: Insulin staining of mouse islets ……. 68

Figure 3.12: The effect of insulin and glibenclamide on islet morphology ……. 71

Figure 3.13: The effect of DMSO on insulin secretion and insulin content …….. 76

Figure 3.14: Insulin secretion from islets isolated from wild-type mice …….. 77

Figure 3.15: Insulin secretion: wild-type vs induced iβ-V59M mice……... 79

Figure 3.16: Insulin content: wild-type vs induced iβ-V59M mice …….. 80

Figure 3.17: Body weight, food intake and water intake ……. 82

Figure 3.18: Blood glucose …….. 83

List of Tables

Table 1:	Average free–fed blood glucose levels for mice bred on a pure C3H/HeJ background vs a mixed genetic background ……	48
Table 2:	Body weight change after pellet implantation - pure C3H/HeJ background vs mixed genetic background ……	49
Table 3:	Blood glucose levels measured 30 minutes after glucose load (IPGTT) …….	55
Table 4:	Comparison between blood glucose levels 30 minutes after a glucose load in an OGTT and IPGTT in male mice ……	57
Table 5:	Comparison between blood glucose levels 30 minutes after a glucose load in an OGTT and IPGTT in female mice ……	57
Table 6:	Blood glucose levels 30 minutes after glucose load in an OGTT ……..	60

List of Abbreviations

K_{ATP} channels	adenosine triphosphate gated potassium channels ……..	8
ATP	adenosine triphosphate ……	8
MgADP	magnesium adenosine diphosphate ……	8
Kir6.2	pore-forming subunit of the K_{ATP} channel;	
	inward-rectifying potassium channel 6.2 ……..	9
SUR1	sulphonylurea receptor ……...	9
MgATP	magnesium adenosine triphosphate ……	12
$[Ca^{2+}]_i$	intracellular free Ca^{2+} concentration ……..	13
GLP-1	glucagon-like peptide-1 ……..	14
GIP	gastric inhibitory polypeptide ……..	14
cAMP	cyclic adenosine monophosphate ……	14
KCNJ11	gene encoding Kir6.2 ……..	15
ABCC8	gene encoding SUR1 ……	15
Kir6.2-V59M mutation	gain-of-function mutation causing neonatal diabetes ……	15
CHI	congenital hyperinsulinism of infancy ……..	15
ND	neonatal diabetes mellitus ……	17
PNDM	permanent neonatal diabetes mellitus ……	17
TNDM	transient neonatal diabetes mellitus ……	17
IC_{50}	the minimal drug concentration that inhibits 50% of its	
	target protein ……...	22
iβ-V59M mouse model	inducible β-V59M mouse model ……..	24

RiP-cre	the expression of the cre recombinase is controlled by the rat insulin promoter ……	24
ER	oestrogen receptor ……..	24
ROSA mouse	ROSA26StopKir6.2-V59M$^{lox/+}$ mouse ……..	25
WT	wild-type ……..	27
$MgCl_2$	magnesium chloride ……..	28
dNTP(s)	deoxyribonucleotide triphosphate(s) ……	28
IPGTT	intraperitoneal glucose tolerance test ……..	31
OGTT	oral glucose tolerance test ……	31
NaCl	sodium chloride ……	31
KCl	potassium chloride ……..	31
$CaCl_2$	calcium chloride ……..	31
NaH_2PO_4	monosodium phosphate ……	31
$NaHCO_3$	sodium bicarbonate ……	31
HEPES	2-[4-(2-hydroxyethyl)piperazin-1-yl]ethanesulfonic acid ……	31
NaOH	sodium hydroxide ……..	31
BSA	bovine serum albumin ……..	31
FBS	foetal bovine serum ……	33
KRB buffer	Tanaka-Robertson-KRB buffer ……	33
KH_2PO_4	monopotassium phosphate ……..	33
$MgSO_4$	magnesium sulfate ……	33
DMSO	dimethyl sulfoxide ……..	33
H_2O_2	hydrogen peroxide ……..	35
Tris	2-Amino-2-hydroxymethyl-propane-1,3-diol ……..	35
HCl	hydrogen chloride ……..	38
Tx	tamoxifen ……	39
ns	not significant ……..	48

Chapter 1: Introduction

1.1 The K_{ATP} channel in the pancreatic β-cell

Among the many different types of ion channels, the adenosine triphosphate (ATP) gated potassium channels (K_{ATP} channels) are of special importance. K_{ATP} channels are unique in that they couple the electrical excitability of the plasma membrane to the cell's metabolic state. This coupling is achieved by the dual regulation of the K_{ATP} channel by the adenosine nucleotides ATP and MgADP: specifically, K_{ATP} channels are inhibited by ATP and activated by MgADP [1].

1.1.1 The discovery of the pancreatic K_{ATP} channel

K_{ATP} channels are found in multiple tissues and play a variety of physiological roles [2]. The pancreatic K_{ATP} channel was discovered in 1984 when Cook and Hales described a K_{ATP} channel which was rapidly and reversibly inhibited by ATP [3]. Almost simultaneously, Ashcroft *et al.* reported that the closure of a channel with similar properties required glucose metabolism [4], and subsequently the two channels were shown to be identical [5]. One of the most important functions of the K_{ATP} channel is to regulate insulin secretion and therefore blood glucose concentrations. It is essential that plasma glucose levels are controlled within narrow limits as failure to do so may result in major health issues: if plasma glucose levels drop below 1-2mM, the main energy source for the brain is lost and

rapid loss of consciousness follows. Conversely, elevated blood glucose levels (>7mM) over long periods can lead to diabetes and its complications - neuropathy, retinopathy, peripheral neuropathy and cardiovascular disease [6]. By regulating insulin secretion from pancreatic β-cells, K_{ATP} channels play a critical role in glucose homeostasis. Their importance is illustrated by the fact that mutations in K_{ATP} channel genes cause severe illnesses like congenital hyperinsulinaemia (loss-of-function mutations) and neonatal diabetes (gain-of-function mutations) [7]. The original treatment for neonatal diabetes was insulin injection but when the causal role of the K_{ATP} channels was discovered ~90% of patients could be transferred to sulphonylurea therapy [8]. This dissertation will compare the effects of sulphonylurea or insulin therapy on islet structure and function in a mouse model of neonatal diabetes. The results have implications for patients suffering from the disease.

1.1.2 The structure of the pancreatic K_{ATP} channel

The human pancreatic β-cell K_{ATP} channel is a hetero-octameric integral membrane protein complex [9, 10] that consists of four Kir6.2 subunits associated with four sulphonylurea receptor (SUR1) subunits (Figure 1.1).

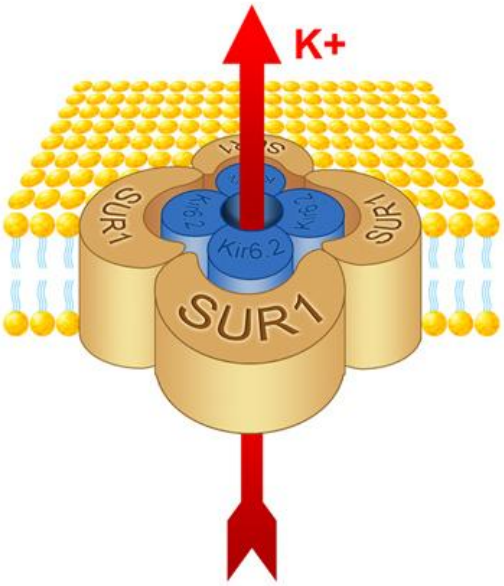


Figure 1.1: The pancreatic K_{ATP} channel

A 3-D cartoon showing the hetero-octameric configuration of the pancreatic K_{ATP} channel. Four Kir6.2 molecules are surrounded by four SUR1 proteins. The pathway for K^+ ions exiting the cell is highlighted in red.

Kir6.2 is an inwardly rectifying potassium channel [11-13] which forms the selective pore for K^+ ions. Each Kir6.2 protein consists of two transmembrane helices connected by a pore loop ('P-loop') (Figure 1.2). This loop contains the selectivity filter of the channel [14, 15]. Additionally, Kir6.2 has a highly structured cytoplasmic domain to which ATP binds, triggering the closure of the K_{ATP} channel [16].

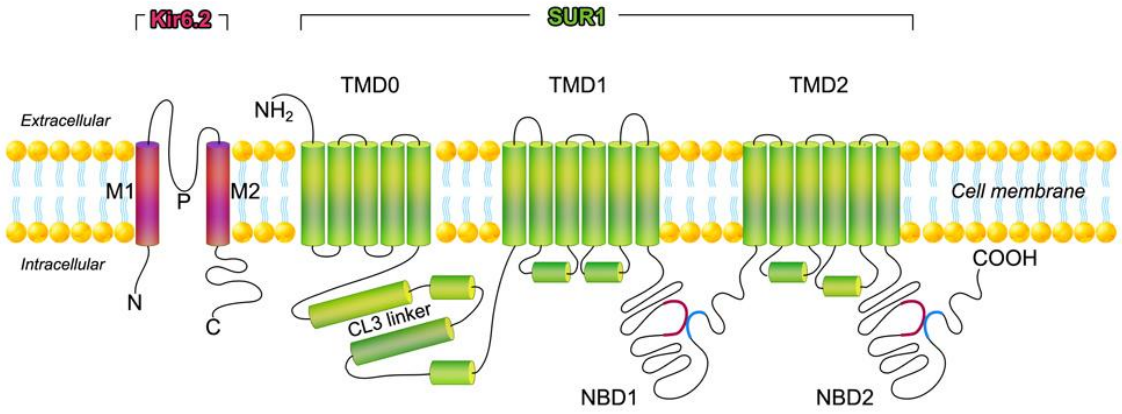


Figure 1.2: Membrane Topology model of SUR1 and Kir6.2

The Kir6.2 subunit is formed by two transmembrane helices (M1 and M2) which are connected by a 'P-loop' which defines the selectivity filter of the channel.
The SUR1 subunit consists of three sets of transmembrane domains (TMD0, TMD1 and TMD2) and 2 nucleotide-binding domains (NBD1 and NBD2). The Walker motifs A (red) and B (blue) are highlighted.

The SUR1 subunit is a transmembrane protein belonging to the ATP-binding cassette (ABC) protein family and its function is to regulate the opening and closing of the Kir6.2 pore [17]. It is formed from three transmembrane domains (TMD0, TMD1 and TMD2) [18, 19]. SUR1 also features two nucleotide-binding domains (NBD1 and NBD2), which contain consensus sequences for nucleotide binding and hydrolysis, known as the Walker A and B motifs (Figure 1.2). Two nucleotide-binding sites are formed by the association of NBD1 and NBD2, such that the Walker A and B motif of one NBD interacts with the ABC signature

sequence of the other NBD. Site 1 is thought to be a high-affinity ATP-binding site, whereas MgADP-binding to Site 2 is thought to stimulate channel opening [15, 18].

The nucleotide regulation of the K_{ATP} channel involves both Kir6.2 (ATP) and SUR1 (MgATP, MgADP), which means that channel activity depends on the energetic state of the cell, and is determined by the balance between ATP inhibition at Kir6.2 and Mg-nucleotide stimulation at SUR1 [20, 21].

Sulphonylurea drugs, such as glibenclamide and tolbutamide, close K_{ATP} channels and are used clinically to treat type 2 diabetes. Conversely, K_{ATP} channel openers like diazoxide activate K_{ATP} channels and are used to treat hyperinsulinism. Both drugs bind to SUR1 and induce a conformational change that results in the closing (sulphonylureas) or opening (diazoxide) of the Kir6.2 pore [17, 20]. The binding sites are not fully established but that for sulphonylureas is known to include residues in cytoplasmic loops 3 and 8 in SUR1 [22].

1.1.3 K_{ATP} channel regulation and insulin secretion

The physiological regulation of the pancreatic K_{ATP} channel is complex. Intracellular nucleotides [3, 23-25] and phosphatidylinositol-4,5-bisphosphate (PIP_2) [26-28] play an important role in its activity. The pancreatic β-cell K_{ATP} channel initiates electrical activity and insulin secretion when glucose concentrations are elevated [4, 29]. It is regulated by glucose metabolism via changes in intracellular ATP and MgADP concentrations. When plasma glucose

levels are low, the MgADP concentration within the pancreatic β-cells is relatively high and ATP levels are low, so that K_{ATP} channels are open. This causes an efflux of potassium ions that generates a negative membrane potential. The hyperpolarization of the cell membrane holds voltage-gated calcium channels closed and keeps intracellular Ca^{2+} $[Ca^{2+}]_i$ below the level needed to stimulate insulin secretion (Figure 1.3A) [4, 6].

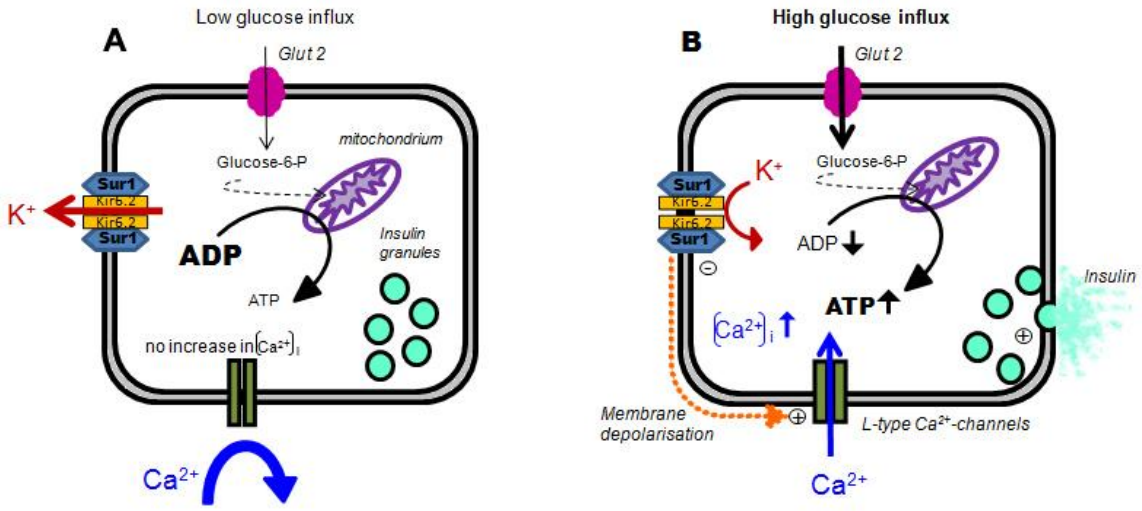


Figure 1.3: The role of the pancreatic K_{ATP} channel in insulin secretion

In case of low glucose metabolism K_{ATP} channels are open which leads to hyperpolarization of the cell membrane and closure of voltage-gated Ca^{2+} channels. Consequently the intracellular concentration of Ca^{2+} $[Ca^{2+}]_i$ remains low and no insulin is secreted (**A**). When glucose metabolism increases, K_{ATP} channels are shut by rising ATP and falling MgADP concentrations, leading to depolarization of the cell membrane and the opening of voltage-gated Ca^{2+} channels. This allows Ca^{2+} to flow into the cell and insulin secretion is triggered (**B**).

When plasma glucose concentration increases, glucose binds to the transmembrane carrier protein Glut2 (glucose transporter 2), which facilitates glucose entry into the pancreatic β-cell. Glucose metabolism increases the concentration of intracellular ATP, and ATP binding to Kir6.2 then leads to the closure of the K_{ATP} channel and depolarization of the β-cell membrane. Consequently, the voltage-gated Ca^{2+} channels open, stimulating $[Ca^{2+}]_i$-dependent electrical activity and Ca^{2+} influx. The rise in $[Ca^{2+}]_i$ then activates insulin release (Figure 1.3B) [4, 6]. This cascade is known as the K_{ATP} channel-dependent or triggering pathway of glucose-induced insulin secretion [30].

The closure of the K_{ATP} channel also enables K_{ATP} channel-independent effects: Glucose metabolism further activates a metabolic amplifying pathway that enhances the triggering action of Ca^{2+} without causing an additional rise in $[Ca^{2+}]_i$. Both triggering and metabolic amplifying pathways contribute to glucose-induced insulin secretion [31]. Hormones, neurotransmitter and secretagogues, such as the incretins glucagon-like peptide-1 (GLP-1) and gastric inhibitory polypeptide (GIP) further potentiate nutrient-induced insulin secretion by stimulating a neurohormonal amplifying pathway that involves elevation of intracellular cyclic adenosine monophosphate (cAMP) [31, 32]. It is known that both L- and K-cells, which secrete GLP-1 and GIP respectively, possess K_{ATP} channels but it seems that these channels do not play a significant physiological role in incretin release [33]. This means K_{ATP} channel mutations are not expected to influence incretin release.

1.2 K_{ATP} channel mutations

Mutations in the genes encoding either the Kir6.2 (KCNJ11) or SUR1 (ABCC8) subunit of the K_{ATP} channel can impair insulin secretion. Loss-of-function mutations cause over-secretion of insulin and result in hypoglycaemia whereas gain-of-function mutations lead to under-secretion of insulin and hyperglycaemia. This condition is known as neonatal diabetes [34-36]. This dissertation will focus on the effect of sulphonylurea and insulin therapy in a mouse model of neonatal diabetes caused by a gain-of-function K_{ATP} channel mutation (Kir6.2-V59M). However, I will first briefly outline what is known about loss-of-function mutations, as this provides important insights into the physiological role of the K_{ATP} channel.

1.2.1 Congenital hyperinsulinism of infancy (CHI)

Congenital hyperinsulinism of infancy (CHI) can be caused by mutations in either the Kir6.2 or the SUR1 subunit [35, 36] and it is characterized by constant and unregulated insulin secretion despite very low plasma glucose levels [37, 38]. CHI occurs in up to one in 50 000 live births [39]. It presents shortly after birth or in early infancy as persistent hypoglycaemia and immediate treatment is crucial in order to prevent irreversible brain injury and mental retardation. K_{ATP} channel mutations in *ABCC8* and *KCNJ11* are the most common cause of CHI and lead to defects in K_{ATP} channel biogenesis and turnover, channel trafficking or the regulation of K_{ATP} channel activity [36, 37, 40]. Pancreatic β-cells from patients with loss-of-function mutations constantly release insulin. This is because their

K_{ATP} channels are always closed leaving the cell membrane in a state of permanent depolarization. Consequently, their voltage-gated Ca^{2+} channels are open all the time, which allows a never-ending influx of Ca^{2+} and thus continuous insulin secretion that is independent of plasma glucose levels (Figure 1.4) [41].

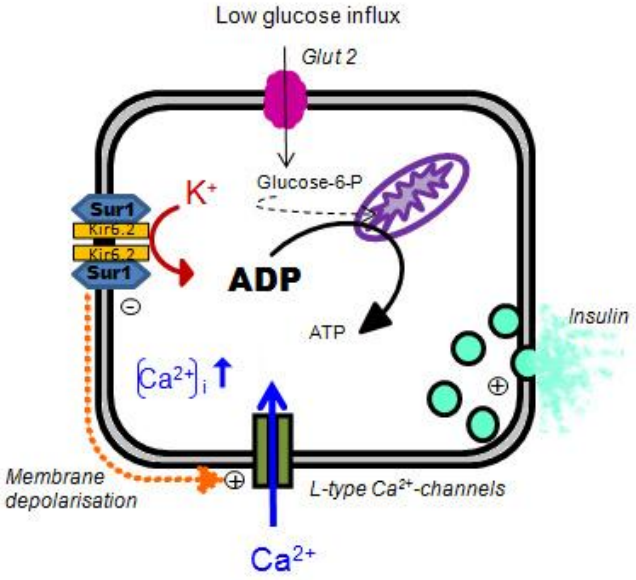


Figure 1.4: Congenital hyperinsulinism of infancy (CHI)

Loss-of-function mutations in either subunit of the K_{ATP} channel prevent the channel from opening even if glucose metabolism is low. As a consequence, the cell is always depolarized, which ensures a constant influx of Ca^{2+} and insulin secretion.

The majority of patients suffering from CHI have recessive mutations in *ABCC8,* the gene that encodes SUR1. Among these mutations, two separate groups, Class I and Class II, were defined according to their effect on protein function. Class I mutations result in the failure of K_{ATP} channels to be transported from the

endoplasmic reticulum to the β-cell plasma membrane. Channels with Class II mutations are trafficked to the membrane but the ability of MgADP to stimulate channel activity is impaired: consequently the mutant K_{ATP} channels do not open even if glucose metabolism is low [42]. Over 150 *ABCC8* mutations causing CHI have been identified. *KCNJ11* mutations associated with CHI are rather rare, however, and only 24 mutations have been reported [35, 43]. These *KCNJ11* mutations also act either by preventing trafficking of K_{ATP} channel to the plasma membrane or by impairing channel opening. However, one Kir6.2 CHI mutation (H259R) has been described that affects both the trafficking and function of the K_{ATP} channel [44].

1.2.2 Neonatal diabetes mellitus (ND)

Neonatal diabetes (ND) is defined by severe insulin-requiring hyperglycaemia that presents within the first 6 months of life. Its phenotype is thus the reverse of CHI. Around 1 out of 200,000 births are affected by ND [34] which can either be permanent (PNDM) or transient (TNDM) [45]. PNDM stays with the patient throughout his life and constant insulin treatment is required, whereas TNDM patients may experience the disappearance of the condition during infancy and its reappearance later in life [7, 46, 47]. Severe gain-of-function K_{ATP} channel mutations may cause neurological symptoms in addition to the diabetes. In the case of intermediate DEND (iDEND) syndrome, patients suffer from neonatal diabetes as well as from mental and motor developmental delay, and flaccid muscles (hypotonia). DEND patients also suffer from epilepsy [34, 48-51]. These

additional symptoms can be explained by the fact that cells containing K_{ATP} channels are spread throughout the whole body and can be found in muscle, brain, heart and endocrine organs (e.g. pancreatic β-cells) [52].

The most common mutations causing neonatal diabetes are in the genes *KCNJ11* (encoding Kir6.2) and *ABCC8* (encoding SUR1). Patients with Kir6.2 mutations are all heterozygotes whereas SUR1 mutations are genetically more heterogeneous, with heterozygous, homozygous, and compound heterozygous all being described [53]. Kir6.2 mutations are most commonly associated with PNDM and SUR1 mutations with TNDM [52].

All ND mutations impair the ability of MgATP to close the K_{ATP} channel. However, the mechanism varies. The most common Kir6.2 mutation occurs at residue R201, which lies in the putative ATP-binding site, and it is therefore thought that this mutation compromises ATP binding. Other mutations, such as the second most common mutation (V59M), are found in parts of the protein that lie far away from the ATP-binding site. It is thought that these may act by impairing the ability of the channel to shut (and because the gate cannot close, the channel is therefore insensitive to ATP) [7, 46, 53].

Many SUR1 mutations causing ND have recently also been found. They are dispersed throughout the whole protein sequence, but concentrated clusters can be seen in the first five transmembrane helices and connecting loops, the third cytosolic linker and NBD2 [19]. They act either by preventing channel closure [54,

55] or by enhancing the ability of Mg-nucleotides to activate the channel [56, 57]. Gain-of-function-mutations leave K_{ATP} channels in a continuously open state that is insensitive to metabolically generated changes in adenine nucleotides. Even if plasma glucose levels rise, the cell membrane stays hyperpolarized, voltage-gated Ca^{2+} channels remain closed, Ca^{2+} influx is prevented and consequently no insulin is secreted (Figure 1.5) [52].

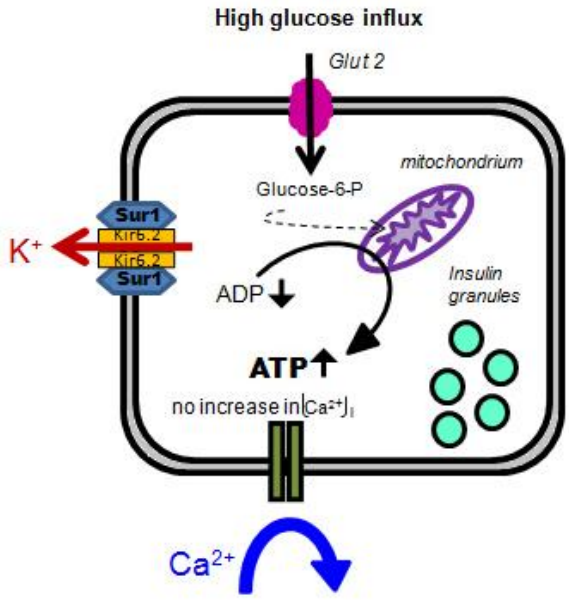


Figure 1.5: Neonatal diabetes (ND)

Gain-of-function mutations in either subunit of the K_{ATP} channel maintain the open state of the channel even if ATP increases within the pancreatic β-cell. As a consequence, the cell membrane remains hyperpolarized even in case of rising plasma glucose levels and insulin secretion is prevented.

1.3 Therapy for diseases caused by K_{ATP} channel mutations

1.3.1 Treatment of congenital hyperinsulinism of infancy (CHI)

As patients with CHI show persistent hypoglycaemia, immediate treatment is crucial in order to keep blood glucose levels normal and prevent brain damage. The most common drug used for CHI therapy is oral diazoxide [37]. This potassium channel activator binds to SUR1 and holds K_{ATP} channels open, hyperpolarising the β-cell and inhibiting insulin secretion. Many dominant inactivating *ABCC8* and *KCNJ11* mutations can be successfully treated with diazoxide [58]. However, diazoxide is often ineffective in recessive CHI, either because the mutant channels fail to respond to the drug or because of a total lack of channels in the plasma membrane [37, 59]. Another drug used for CHI therapy is somatostatin, which inhibits insulin release downstream of K_{ATP} channel closure, at the level of exocytosis [60-62]. This therapy is not recommended for treating children because multiple injections are required each day [63].

If drug therapy fails surgery is considered [64]. Up to 90% of the pancreas may need to be removed. Surgery is very effective at reducing insulin secretion but in the long term may lead to diabetes and the patient also needs to take pancreatic enzyme supplements [53].

1.3.2 Treatment of neonatal diabetes (ND)

In the past, ND patients were treated with daily insulin injections, as their clinical characteristics suggested an unusually early-onset form of type 1 diabetes, for which insulin therapy is essential [65]. However, when the causal role of the K_{ATP} channels was discovered in 2004, it was evident that it might be possible to close the open K_{ATP} channels in ND patients with oral sulphonylurea drugs and so stimulate insulin secretion. This proved to be the case and ~90% of patients have been transferred to sulphonylurea therapy [8]. Sulphonylurea drugs, such as tolbutamide or glibenclamide, are specific K_{ATP} channel blockers [66] and therefore stimulate insulin secretion. As a consequence the clinical condition of patients greatly improves: fluctuations in blood glucose levels are much reduced [67] and hypoglycaemic episodes are significantly less common. Plasma glucose levels are also much lower, as can be seen by the decreased HbA1C levels [8]. This improvement in glycaemic control is predicted to lower the risk of diabetic complications [68, 69]. In a few cases, the extra-pancreatic symptoms like muscle hypotonia and motor and developmental delay are also improved [70-72]. In addition to these clinical benefits, the patients' quality of life is improved as they no longer need injections but simply a pill once or twice a day.

In healthy individuals, an oral glucose load triggers insulin secretion more effectively than an isoglycaemic intravenous glucose infusion. This phenomenon is known as the ‘incretin effect’ as it is mediated by the incretin hormones GLP-1 and GIP in response to the presence of glucose in the gut lumen [73-75]. GLP-1 is

released from enteroendocrine L-cells in the distal ileum and colon [76] and GIP is released from enteroendocrine K-cells in the proximal small intestine [77]. These hormones stimulate the pancreatic β-cell to produce intracellular cyclic adenosine monophosphate (cAMP) [78, 79], which promotes exocytosis of secretory granules and therefore potentiates insulin release [31, 32]. Patients with type 2 diabetes show a reduced incretin effect [80], as do ND patients treated with insulin. However, when ND patients are treated with sulphonylureas, the incretin response is restored [8], as incretin action requires a K_{ATP}-dependent increase in intracellular Ca^{2+}. This may explain why these hormones have no effect on patients with K_{ATP} channel mutations in the absence of sulphonylureas therapy. Closure of K_{ATP} channels by sulphonylureas leads to an increase in intracellular Ca^{2+} and incretins are then able to trigger insulin secretion [65].

The sulphonylurea drugs glibenclamide and tolbutamide are very successful at treating patients with K_{ATP} channel mutations that cause neonatal diabetes [81]. The average glibenclamide dose given to patients is 0.45mg/kg/day (range: 0.05 to 1.5mg/kg/day). Channels carrying Kir6.2 or SUR1 mutations are inhibited between 72-96% by tolbutamide concentrations (0.2-0.5mM) that maximally block wild-type channels [8, 52]. In the case of the Kir6.2-V59M mutation, a concentration of 0.2mM tolbutamide results in approximately an 80% block of the K_{ATP} current [82]. Glibenclamide is most commonly used to treat patients suffering from neonatal diabetes. A decrease in sensitivity to glibenclamide can also be seen in mutations in either subunit of the K_{ATP} channel. In pancreatic β-cells expressing the Kir6.2-V59M mutation the IC_{50} for glibenclamide is shifted from

2.1±0.2nM for the wild-type channel to 7.5±3.5nM for the mutant channel. Furthermore, while a 100nM concentration of glibenclamide fully blocks the wild-type channel, 10% of current remains for the Kir6.2-V59M channel with the same dose (P. Proks, *unpublished*). Even at high doses of sulphonylurea, transitory diarrhea is the only side effect that has been reported (apart from hypoglycaemia) [8]. Anecdotal evidence seems to suggest that, unlike type 2 diabetes mellitus patients on glibenclamide, glibenclamide-treated neonatal diabetes patients lose body weight [83, 84].

1.4 The V59M mouse model

A few years ago Girard *et al* created a novel Cre-lox mouse model (β-V59M) with a specific gain-of-function mutation (Kir6.2-V59M), which is the most common cause of iDEND [82]. These mice express a mutant Kir6.2 subunit in all pancreatic β-cells. Human patients are heterozygous for this mutation and, fortuitously, transgenic mice expressed comparable levels of normal (wild-type) and Kir6.2-V59M mRNA in pancreatic islets, which makes the mouse model comparable to the human patients in terms of gene expression. When the mutant gene was activated prior to birth, β-V59M mice developed severe diabetes soon after birth and by 5 weeks of age blood glucose levels were heavily elevated and plasma insulin levels were undetectable. Isolated islets showed a decrease in insulin secretion and a smaller glucose-induced increase in intracellular Ca^{2+}, due to a reduced K_{ATP} channel sensitivity to ATP inhibition. Their islets also showed reduced insulin content and β-cell area, as well as a change in islet morphology.

Expression of the V59M mutation in pancreatic β-cells alone was therefore shown to reflect the neonatal diabetes phenotype seen in human patients. However, it was difficult to use this early-onset hyperglycemic mouse model to investigate the effects of sulphonylurea therapy because the islets were largely destroyed before the mouse was old enough for a subcutaneous slow-release drug pellet to be implanted.

In order to explore the effect of diabetes and of different therapies, we therefore used adult mice. An inducible mouse model (iβ-V59M) was created by crossing RIP-cre-ER mice [85] with ROSA-V59M mice [82]. In this project, I focused on the effect of neonatal diabetes in the adult mouse. I compared the influence of insulin and sulphonylurea treatment on blood glucose levels, glucose tolerance, insulin secretion, and islet and β-cell distribution within the pancreas.

Chapter 2: Methods and Materials

2.1 A mouse model of Neonatal Diabetes - the inducible β-V59M (iβ-V59M) mouse

2.1.1 Generation of iβ-V59M mice

Mice which selectively express a gain-of-function mutation in the pore-forming subunit of the K_{ATP} channel (Kir6.2-V59M) in pancreatic β-cells (iβ-V59M) were generated using a Cre-lox approach.

The Kir6.2-V59M gene, preceded by a loxP-flanked STOP sequence and followed by a flippase (FLP) recombinase target (FRT)-flanked internal ribosome entry site (IRES) GFP cassette, was targeted to the ROSA26 locus to ensure that a single copy of the mutant Kir6.2 gene was expressed from a known location [82]. The endogenous ROSA promoter was used to prevent excess gene expression.

To generate mice which express the Kir6.2-V59M mutation specifically in insulin-secreting cells, ROSA26StopKir6.2-V59M$^{lox/+}$ mice (ROSA mice) were crossed with mice expressing a modified version of the Cre recombinase fused to the oestrogen receptor (ER) ligand-binding domain under the control of a rat insulin promoter (RIP-cre-ER mice) [85]. These mice were kindly provided by Dr Yuval Dor (Jerusalem). Despite being expressed throughout development, the Cre-ER

fusion protein remains inactive due to heat-shock proteins binding to the ER ligand-binding protein. Upon addition of the synthetic steroid tamoxifen, the Cre-ER fusion protein becomes active and mediates the excision of the loxP-flanked STOP sequence in the nucleus (Figure 2.1) [86].

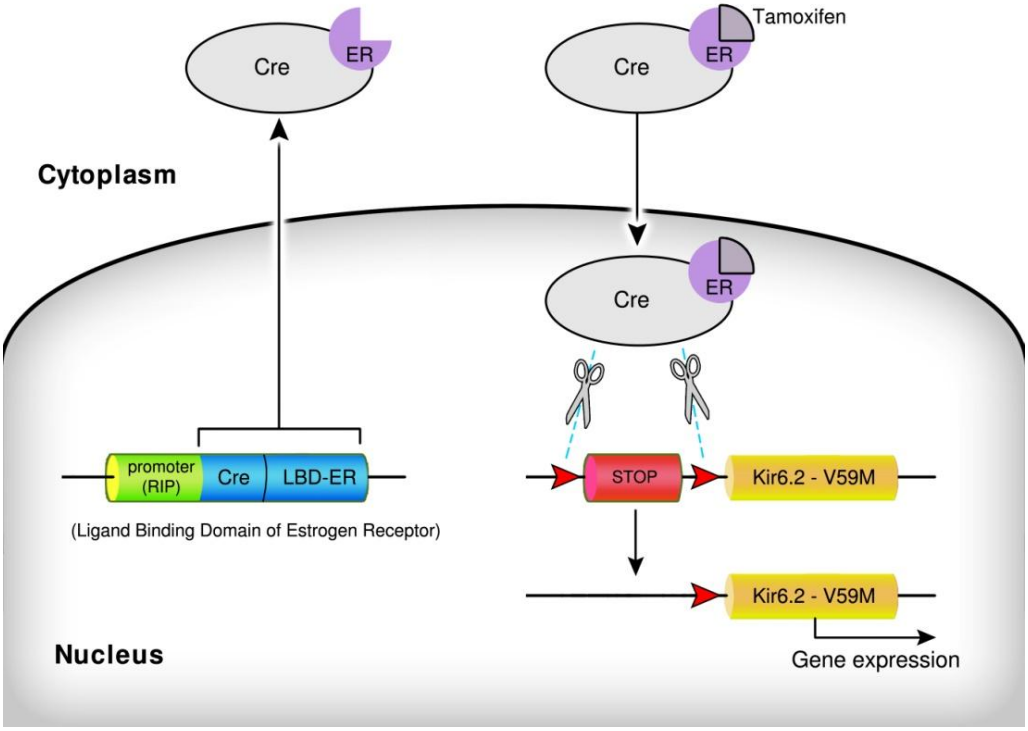


Figure 2.1: The cre ER-loxP system

Left: In the absence of tamoxifen the fusion complex, comprised of the rat insulin promoter (RIP) and the ligand-binding domain of the oestrogen receptor (LBD-ER), is inactivated and confined to the cytoplasm.

Right: When activated by tamoxifen, the cre-ER fusion protein moves to the nucleus, where the loxP-flanked STOP sequence is cut out and the Kir6.2-V59M mutation is expressed in the pancreatic β-cells.

The majority of experiments were conducted using mice bred on a mixed genetic background (C57Bl/6, C3H/HeJ, BALB/c). Mice bred on a pure C3H/HeJ genetic background were only used to a limited extent because of reduced breeding efficiency.

2.1.2 Genotyping

Genotypes were identified by PCR using genomic DNA isolated from ear biopsies (Maxwell 16; Promega). The presence of the Kir6.2-V59M mutant gene was confirmed using the following set of primers:

P1: 5′-AAAGTCGCTCTGAGTTGTTATC-3′,
P2: 5′-GATATGAAGTACTGGGCTCTT-3′,
P3: 5′-GCATCGCCTTCTATCGCCT-3′.

These primers amplify a 590-bp amplicon from the WT (wild-type) ROSA26 allele but a 460-bp product from the targeted allele.
The presence of the RIP-cre ER gene was confirmed by the amplification of a ~230-bp product, using Cre primers:

5'-cre: 5'-ACGAGTGATGAGGTTCGCA-3',
3'-cre: 5'-ATGTTTAGCTGGCCCAAATGT-3'.

The PCR was carried out in 25µl reactions in a GeneAmp2700 thermocycler using 20ng genomic DNA template, 10µM primer, 15µl DreamTaq™ Green PCR Master Mix (Fermentas) containing DreamTaq™ DNA polymerase, optimized DreamTaq™Green buffer, $MgCl_2$ and dNTPs, and nuclease free water. For both sets of primers PCR conditions were 95°C for 4 minutes, followed by 38 cycles of 95°C for 30 seconds, 54°C for 45 seconds and 72°C for 1 minute 30 seconds. This was followed by a final extension at 72°C for 10 minutes.

2.1.3 Animal care

All experiments were conducted in accordance with the UK Animals Scientific Procedures Act (1986) and University of Oxford ethical guidelines. Mice were housed in same-sex littermate groups of 2-8 animals. Their room was temperature and humidity controlled with a 12h light-dark cycle (lights on at 7am). Regular chow food containing 61% carbohydrates, 27% protein and 12% fat (Special Diet Services, RM3) was freely available, except during overnight fasting for glucose tolerance tests (see below). As untreated induced iβ-V59M mice are polyuric, they were maintained on high absorbency bedding. Littermates were used for all studies.

2.1.4 Gene induction and pellet implantation

Kir6.2-V59M expression was induced in 12-week-old mice by a single subcutaneous injection of 0.4ml of 20mg/ml tamoxifen (Sigma) in corn oil (Sigma).

Blood glucose levels were monitored daily, using the FreeStyle Lite Blood Glucose Monitoring System (Abbott). This glucose meter only displayed readings between 1.1mM and 27.8mM. Blood glucose results <1.1mM were documented as 1mM and blood glucose results exceeding 27.8mM were documented as 28mM. Once blood glucose levels reached 20mM (2-3 days after tamoxifen induction), animals were implanted subcutaneously with one of the following pellets under general anaesthesia (2% isoflurane, Animal Care Ltd):

- 60-day slow-release glibenclamide pellet (25mg, Innovative Research of America).
- Placebo pellet which contained the same vehicle as the 60-day slow-release glibenclamide pellet but no drug (Innovative Research of America).
- Insulin pellets with a release rate of ~0.1U/24h/implant for >30 days (LinShin Canada Inc.). The number of insulin pellets implanted was determined according to body weight. Mice weighing between 20g and 30g were implanted with two pellets while the maximum of three pellets was implanted in those of body weight between 30g and 40g. If blood glucose levels exceeded 20mM between five and fourteen days after implantation, an additional pellet was administered immediately.
- Placebo pellets which contained the same vehicle as the insulin pellets but no drug (LinShin Canada Inc.). The number of pellets implanted was calculated as previously stated for the insulin pellets.

Wild-type mice or mice expressing only the floxed Kir6.2-V59M gene (ROSA mice) were used as controls. They were injected with tamoxifen and implanted with glibenclamide, insulin or placebo pellets in the same way as iβ-V59M mice.

In a different experiment, the effect of glibenclamide therapy on water and food intake as well as body weight was examined. Wild-type mice were implanted with 21-day slow release glibenclamide pellets (2.5mg, Innovative Research of America). Placebo pellets contained the vehicle but no glibenclamide.

2.1.5 Mouse body mass and blood glucose monitoring

Mouse body mass was measured on scales calibrated to 0.01g. Free fed plasma glucose levels were usually monitored daily or on alternate days between 2 and 3pm, using the FreeStyle Lite Blood Glucose Monitoring System (Abbott). Measurements were made on iβ-V59M mice and control mice for up to 4 weeks before gene induction or pellet implantation and for up to 4 weeks after pellet implantation.

2.1.6 Food and water intake experiments

Food hoppers and water bottles of wild-type mice were weighed 3 times a week and the average food and water intake over the preceding 7 days was calculated. Measurements were made each week for 4 weeks prior to pellet implantation and for 4 weeks after pellet implantation.

2.2 Glucose tolerance tests

To investigate the response to an administered glucose load an intraperitoneal glucose tolerance test (IPGTT) and an oral glucose tolerance test (OGTT) were carried out. Following a 16-18 hour overnight fast, mice were weighed and Lidocaine EMLA topical anaesthetic cream (AstraZeneca) was administered to the tail. Fifteen minutes after applying the local anaesthetic, an initial blood sample was collected via tail vein puncture to obtain a baseline glucose measurement (T_0). Mice were then challenged with a glucose load of 2g/kg body weight, administered intraperitoneally (IPGTT) or by oral gavage (OGTT). Blood glucose levels were measured 30, 60 and 120 minutes after glucose administration using the FreeStyle Lite Blood Glucose Monitoring System (Abbott).

Insulin treatment increased the risk of severe hypoglycaemia. Therefore, induced iβ-V59M mice implanted with insulin pellets were only fasted for 4-5 hours prior to glucose tolerance tests.

2.3 Pancreatic islet studies

2.3.1 Isolation of pancreatic islets using enzyme digestion

Hanks' buffer containing 137mM NaCl, 5.6mM KCl, 1.2mM $MgCl_2$, 2.56mM $CaCl_2$, 1.2mM NaH_2PO_4, 4.2mM $NaHCO_3$, 10mM HEPES, pH 7.4 with NaOH, plus 3mM Glucose and 0.5% bovine serum albumin (BSA) was used as the media

throughout the procedure. Mice were killed by cervical dislocation. For pancreas digestion, 2ml of liberase TL Research Grade (Roche) solution (0.375mg/ml in Hanks' solution) were injected into the bile duct after closing the exit to the duodenum with a surgical string (Figure 2.2).

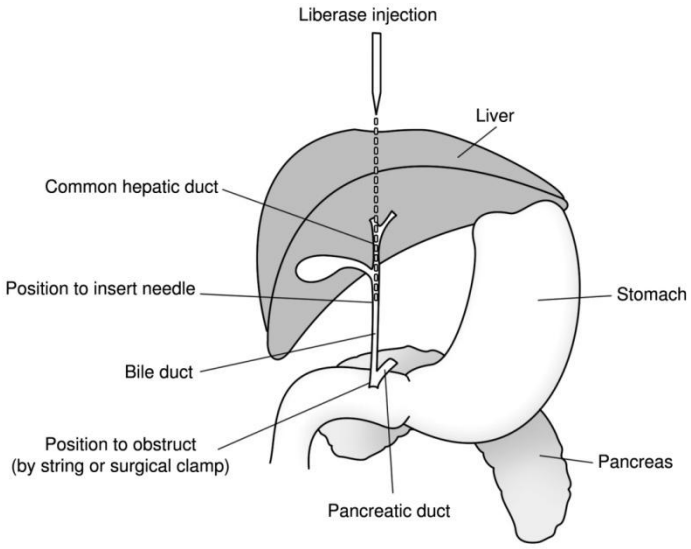


Figure 2.2: Liberase injection into the bile duct

Image showing the needle insertion point in the bile duct and the position at which the exit to the duodenum was closed.

After injection, the inflated pancreas was carefully dissected, placed in 2ml of liberase solution and incubated at 37°C for 14 minutes. The digested pancreas was washed twice with 20ml of ice-cold Hanks' solution and centrifuged at 2000rpm for 2 minutes. Single islets were then handpicked several times under the microscope in order to obtain pure islets. Cells were maintained in RPMI 1640 medium containing 10mM glucose (Invitrogen) supplemented with 1% penicillin and 10% fetal bovine serum (FBS) at 37°C in a humidified atmosphere at 5% CO_2. Isolated pancreatic islets were used the following day for additional experiments.

2.3.2 Insulin secretion experiments

Following overnight incubation 50 pancreatic islets were placed on top of an 8µm pore diameter filter membrane mounted inside Swinnex filter holder chambers (Millipore) and perifused at 37°C at a rate of 1ml/min with Tanaka-Robertson-KRB buffer (KRB buffer) containing 120mM NaCl, 5.5mM $CaCl_2$, 1.2mM KH_2PO_4, 4.7mM KCl, 25mM $NaHCO_3$, 1.2mM $MgSO_4$, 10mM HEPES, pH 7.4 with NaOH, plus 0.1% BSA and glucose as indicated below. A 1M stock solution of tolbutamide was made in dimethyl sulfoxide (DMSO, Sigma), and diluted as required. Islets from mice implanted with placebo, glibenclamide (25mg) or insulin pellets were pre-perifused in 2mM glucose KRB buffer for 30 minutes. They were then perifused for 10 minutes in 2mM glucose KRB buffer, followed by 20 minutes in 20mM glucose KRB buffer and 10 minutes in 20mM glucose KRB buffer containing 0.5mM tolbutamide. The perfusate was collected every minute into separate tubes. At the end of the experiment, islets were placed in 2ml acidified

ethanol solution (95% ethanol, 5% acetic acid) and left at -20°C for two days to ensure complete lysis of the islets. This enabled measurement of the total insulin content. Insulin was then measured using a mouse insulin ELISA kit (Mercodia).

2.3.3 Insulin secretion experiments using static incubation

Isolated islets from 14-week old wild-type mice were starved in 2mM glucose KRB buffer at 37°C for 30 minutes after overnight incubation in RPMI medium containing 10mM glucose. Groups of five islets were then incubated for 1 hour at 37°C in 2ml KRB buffer containing the following additions:

- 2mM, 5mM, 10mM or 20mM glucose.
- 2mM, 5mM, 10mM or 20mM glucose plus 20nM glibenclamide.
- 2mM, 5mM, 10mM or 20mM glucose plus 2µM glibenclamide.
- 2mM, 5mM, 10mM or 20mM glucose plus 20µM glibenclamide.

Islets from iβ-V59M mice were also used for static incubation experiments. 14-week-old mice were induced with tamoxifen. When blood glucose levels reached 20mM mice were kept an additional day to ensure that the Kir6.2-V59M mutation was expressed in the pancreatic K_{ATP} channel before the islets were isolated. Islets from diabetic mice were incubated overnight and fasted in the same way as wild-type islets. Groups of five islets were then incubated for 1 hour at 37°C in 2ml KRB buffer containing the following additions:

- A 2mM or 5mM glucose.
- A 2mM or 5mM glucose plus 20nM glibenclamide.
- A 2mM or 5mM glucose plus 2µM glibenclamide.
- A 2mM or 5mM glucose plus 20µM glibenclamide.

Immediately after incubation, islets were transferred into 0.5ml acidified ethanol solution (95% ethanol, 5% acetic acid) and stored at -20°C overnight. Subsequently, 1ml of solution of each condition was collected and centrifuged at 3000rpm for 5 minutes. A final volume of 0.5ml supernatant was stored at -20°C. The following day insulin was measured using a mouse insulin ELISA kit (Mercodia).

2.4 Immunohistochemistry

Pancreata were dissected and fixed in 10% formaldehyde in phosphate-buffered saline (PBS) at 4°C. The specimens were then washed in PBS and dehydrated in 70%, 90% and 100% ethanol followed by chloroform. After wax embedding, 5 sections (2µm thick) from each pancreas, taken at 100µm intervals from one another, were mounted on slides, dewaxed in Xylene and successively rehydrated in 100% ethanol, 70% ethanol and distilled water. In order to block endogenous peroxidase activity, the sections were placed in freshly prepared 0.3% H_2O_2 solution for 30 minutes. The blocking solution was then washed away with water followed by a wash in 0.1M Tris HCl buffer. Non-specific binding of antibodies was blocked by incubation with non-immune animal serum (swine serum, diluted 1/20

in Tris HCl buffer) for 20 minutes. The primary antibody against insulin (raised in guinea pig, diluted 1/1000 in Tris HCl buffer) was then applied and incubated at 4°C overnight. The following day the sections were washed in 0.1M Tris HCl buffer and peroxidase (HRP) labeled anti-guinea pig antibody (Dako, diluted 1/50) was administered for 30 minutes. After another wash, insulin-positive cells were stained with 3,3'-diaminobenzidine (DAB, Sigma) and other tissues counterstained with Mayer's haematoxylin solution (Sigma). Aquatex (VWR) was used as a mounting medium (Figure 2.3).

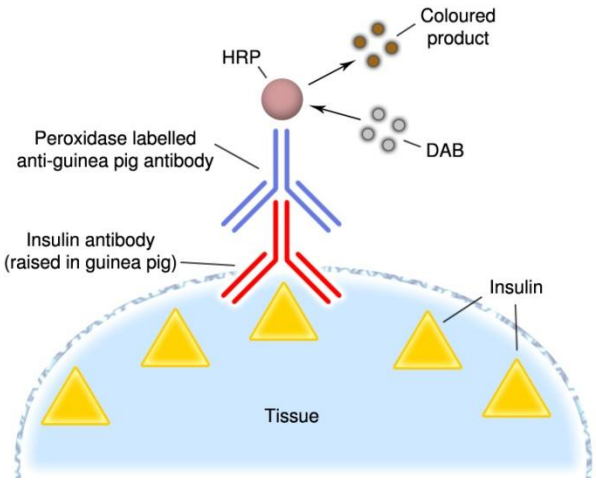


Figure 2.3: Insulin staining using indirect immunohistochemistry

The antibody against insulin binds to the hormone insulin produced in the pancreatic β-cell. As the insulin antibody was raised in guinea pig, a specific peroxidase (HRP) labeled anti-guinea pig antibody binds to it. HRP catalyzes the conversion of DAB into a polymerised brown product which can be detected visually under the microscope.

Images of islets and of the entire pancreatic section were taken with a Nikon digital camera. Images were then imported into a Zeiss LSM-510 software package and analyzed using the histogram tool. For quantification of β-cell area, all 5 sections from each pancreas were analyzed for 2-3 animals of each genotype and each treatment (wild-type mice implanted with placebo, insulin and glibenclamide treated mice and induced iβ-V59M mice implanted with placebo). Usually this amounted to a total of approximately 150 islets. Total islet cross-sectional area, the percentage of cross-sectional area which comprised β-cells (as identified by insulin staining), islet number (per cm^2) and individual islet size (cross-sectional area) were quantified.

2.5 Statistical analysis

All statistical analyses were performed using GraphPad Prism 5 (GraphPad Software, USA). Data are presented as mean values ± SEM of indicated (n) numbers of experiments. Pancreatic islet morphology and insulin content of control mice and induced iβ-V59M mice treated with placebo, glibenclamide or insulin, as well as static incubation experiments in different glucose solutions were compared using a one-way ANOVA followed by *post hoc* Bonferroni's multiple comparisons tests. The same tests were used to compare blood glucose levels of control mice and induced iβ-V59M mice treated with placebo, glibenclamide or insulin pellets which were measured 30 minutes after a glucose load in an IPGTT or an OGTT. Glucose tolerance tests and static incubation experiments on wild-type and induced iβ-V59M mice were compared using a two-way ANOVA followed by *post*

hoc Bonferroni's multiple comparisons tests. This test was also used to analyze the effect of glibenclamide on body weight and blood glucose levels. Peak blood glucose levels in an IPGTT and an OGTT were compared using an unpaired t-test which was also used to analyze average free-fed blood glucose levels measured in mice bred on different genetic backgrounds. Differences between groups were considered significant at $P<0.05$. All analyses were carried out using two-tailored tests.

Chapter 3: Results

3.1 Iβ-V59M mouse model: blood glucose homeostasis and body weight

3.1.1 Expression of the Kir6.2-V59M mutation causes diabetes

The Kir6.2-V59M gene was introduced into the ROSA26 locus and the mutation was expressed under the control of the endogenous ROSA promoter [82]. These floxed Kir6.2-V59M mice were crossed with RIP-cre ER mice [85] which resulted in a mouse model expressing the Kir6.2-V59M mutation specifically in the pancreatic β-cells (iβ-V59M). Gene expression was activated with tamoxifen (Tx). In order to determine the phenotype of induced iβ-V59M mice and their response to glibenclamide and insulin treatment, 12-week old male and female mice were injected with tamoxifen. Within the following 2-3 days, free-fed blood glucose levels rose rapidly up to ≥ 20mM (Figures 3.1, 3.2). No change in free-fed blood glucose levels was seen in control animals injected with tamoxifen (Figures 3.1, 3.2).

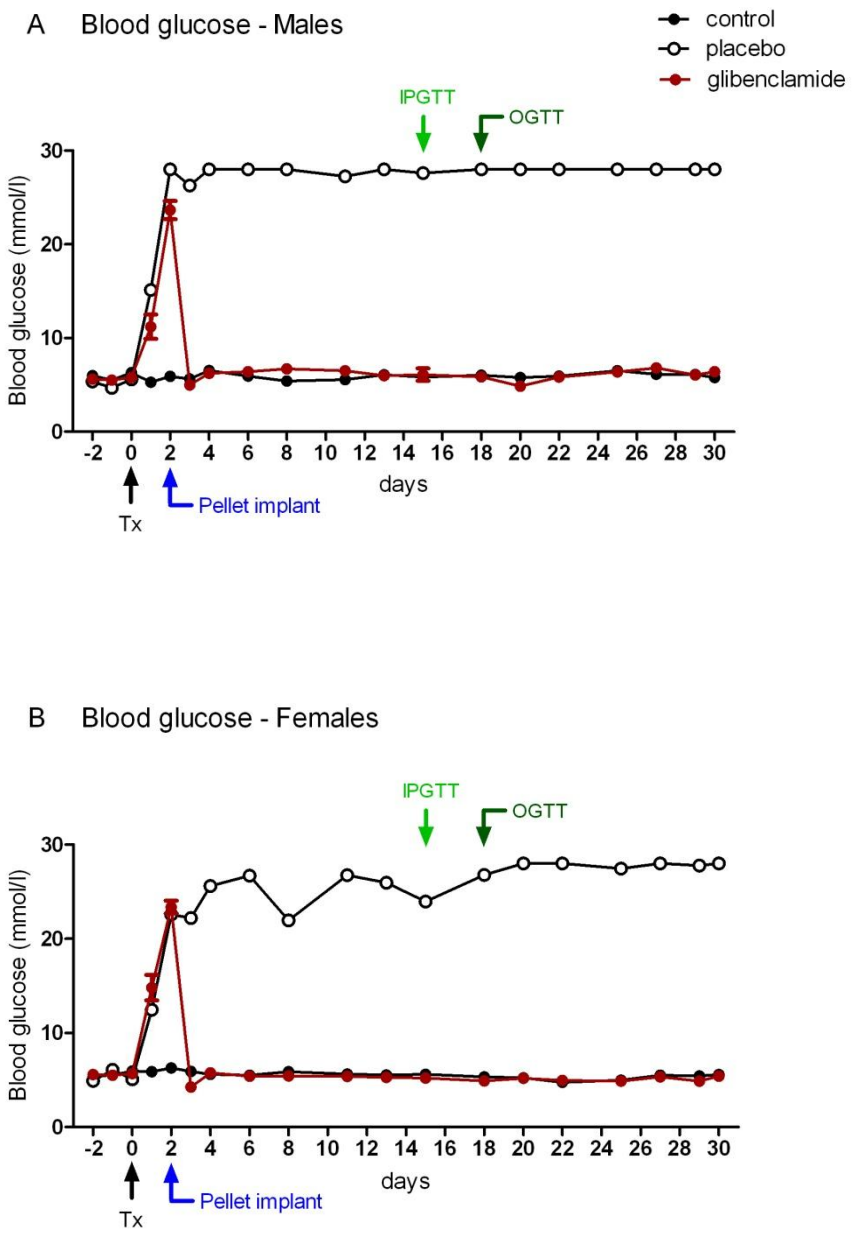


Figure 3.1: Free-fed blood glucose - glibenclamide treatment

Average free-fed blood glucose concentrations of male (**A**) and female (**B**) mice measured over 2 days preceding gene induction and up to 4 weeks after placebo or glibenclamide pellet implantation (at day 2). Tamoxifen (Tx) was given at day 0 to induce gene expression. Results are mean ± SEM for control mice (●, n=6 males and 6 females) and induced iβ-V59M mice implanted with glibenclamide pellets (●, n=9 males and 10 females) and mean for induced iβ-V59M mice implanted with placebo pellets (○, n=2 males and 2 females). IPGTT = intraperitoneal glucose tolerance test; OGTT = oral glucose tolerance test.

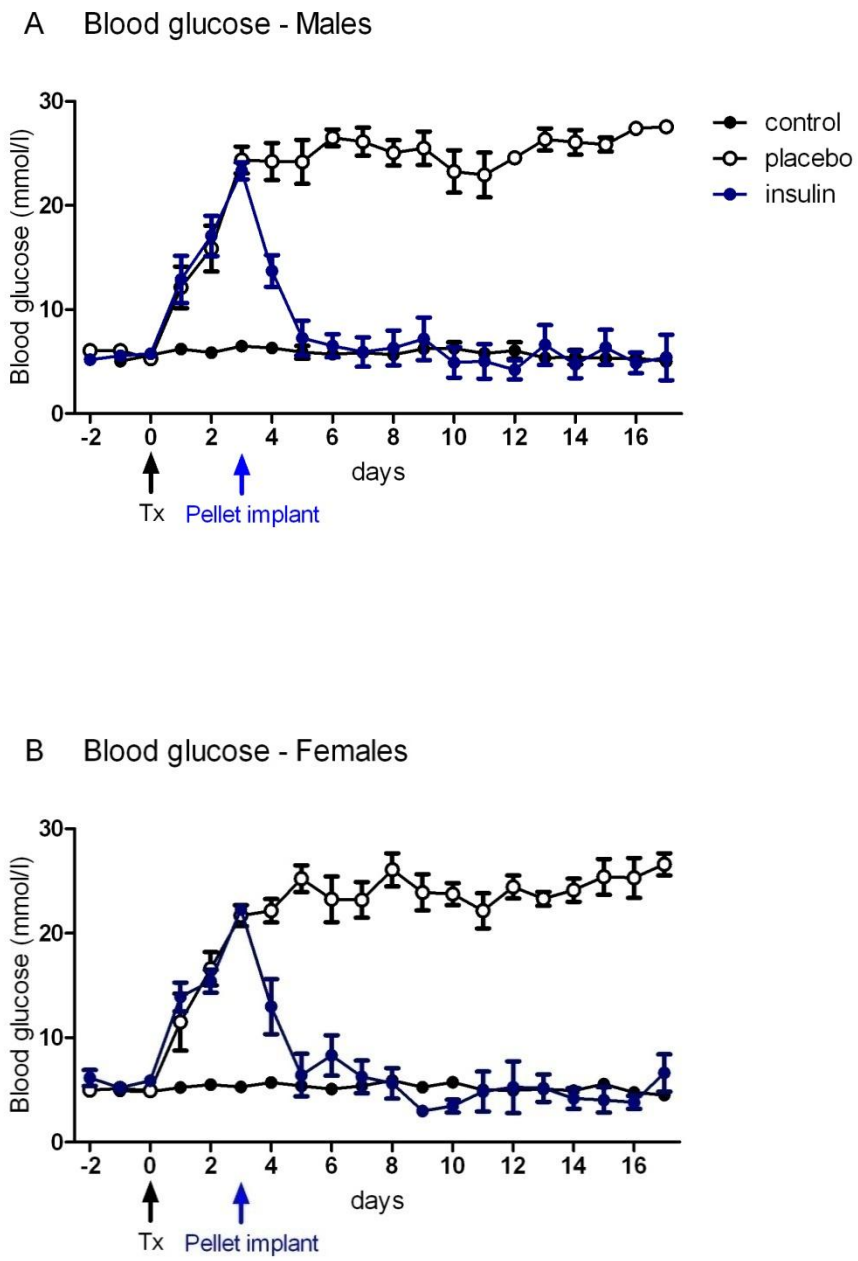


Figure 3.2: Free-fed blood glucose - insulin treatment

Average free-fed blood glucose concentrations of male (**A**) and female (**B**) mice measured over 2 days preceding gene induction and up to 2 weeks after placebo or insulin pellet implantation (at day 3). Tamoxifen (Tx) was given at day 0 to induce gene expression. Results are mean ± SEM for control mice (●, n=6 males and 6 females), induced iβ-V59M mice implanted with placebo pellets (○, n=5 males and 6 females) and induced iβ-V59M mice implanted with insulin pellets (●, n=11 males and 11 females).

3.1.2 Glibenclamide and insulin therapy normalize blood glucose levels

Patients suffering from neonatal diabetes were originally treated with daily insulin injections. However, when it was discovered that K_{ATP} channel mutations cause neonatal diabetes, the majority of patients were transferred to sulphonylurea therapy (e.g. glibenclamide, tolbutamide) [8].

To compare the effect of glibenclamide and insulin therapy on glucose homeostasis, 12-week old male (n=9) and female (n=10) induced iβ-V59M mice were implanted with a subcutaneous slow-release glibenclamide pellet (25mg/60 days), once blood glucose levels exceeded 20mM. For a mouse of 25g and release duration of 60 days a 25mg pellet corresponds to a dose of ~17mg/kg/day, which is ~40 times higher than the average dose given to a neonatal diabetes patient (0.45mg/kg/day) [8].

In previous studies, Shimomura *et al* (unpublished) treated induced iβ-V59M mice with 21-day slow-release pellets containing 0.25mg glibenclamide which corresponds to a dose of 0.5mg/kg/day. Although this glibenclamide concentration is within the range used to treat patients with neonatal diabetes (0.05-1.5mg/kg/day) [8], blood glucose levels of implanted mice were somewhat higher than controls and they became increasingly diabetic after 2 weeks.

Treatment with high-dose glibenclamide pellets proved to be more successful. Two days after gene induction, blood glucose levels in male mice rose to 23.7 ± 1.0mM (n= 9) (Figure 3.1A). Glibenclamide therapy led to a rapid decrease in blood glucose to 5.0 ± 0.2mM the following day. Free-fed blood glucose levels were well controlled over the next 4 weeks and averaged 6.1 ± 0.1mM which is comparable to that measured in control mice (6.0 ± 0.1mM, n=6). Induced and placebo-treated iβ-V59M mice were severely hyperglycemic (average: 27.8mM, n=2) for 4 weeks. Similar results were obtained for female induced iβ-V59M treated with glibenclamide (n=10), or placebo pellets (n=2) and for control mice implanted with placebo pellets (n=6) (Figure 3.1B).

Figures 3.1A and 3.1B also show that glucose tolerance tests, performed 2 weeks after pellet implantation, had no subsequent effect on free-fed blood glucose levels.

A second set of induced iβ-V59M mice was treated with insulin once blood glucose levels had risen above 20mM. Blood glucose levels in male iβ-V59M mice reached 23.3 ± 0.8mM (n=11) 3 days after tamoxifen injection. Insulin treatment (0.1U/24h/30days) normalized blood glucose levels to 7.3 ± 1.7mM within 2 days after treatment and plasma glucose levels averaged 6.4 ± 0.6mM over the next 2 weeks. However, fluctuations in blood glucose levels were more pronounced than with glibenclamide therapy: it is possible this is due to differences in eating patterns. Induced and placebo-treated iβ-V59M mice became severely hyperglycemic (25.4 ± 0.4mM, n=5) (Figure 3.2A). Blood glucose levels in control

mice were unaffected by placebo pellet implantation, averaging 5.7 ± 0.1mM (n=6) during the 2 weeks after implantation. Female mice in which Kir6.2-V59M expression was induced with tamoxifen and which were then treated with insulin or placebo and control mice implanted with placebo pellets showed similar results to male mice (Figure 3.2B).

3.1.3 Glibenclamide and insulin therapy have no effect on body weight

It has been reported that neonatal diabetes patients treated with glibenclamide experience a decrease in body weight. By contrast, patients with type 2 diabetes mellitus gain body weight when treated with sulphonylureas [83, 84]. Furthermore, patients on insulin therapy also gain weight as insulin is a putative adiposity signal to the brain [87].

Induced male and female iβ-V59M mice were individually weighed on alternate days for up to 4 weeks after glibenclamide or insulin pellet implantation in order to examine if these agents caused loss or gain of body weight. Figures 3.3A and 3.3B show that neither the body weight of male nor that of female mice was affected by the drug glibenclamide. Similar results were obtained for animals treated with insulin pellets (Figures 3.4A and 3.4B).

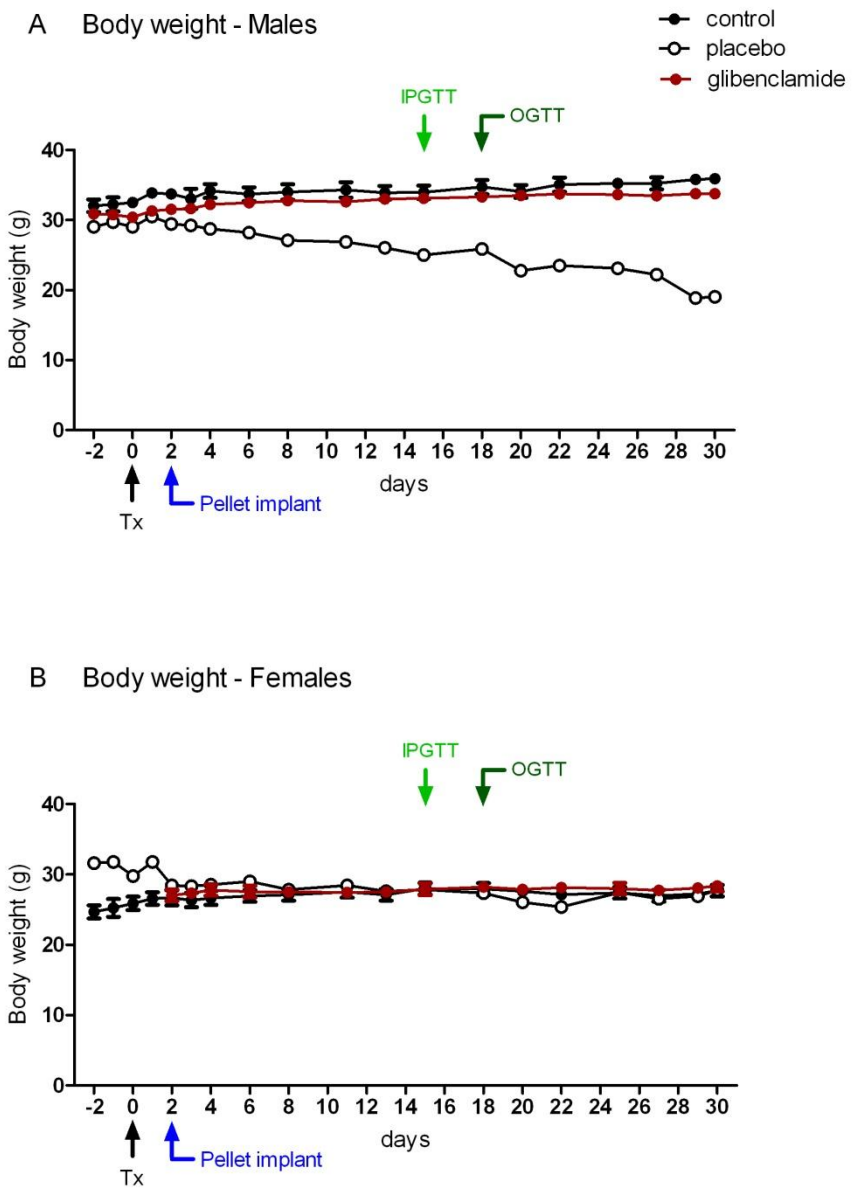


Figure 3.3: Body weight - glibenclamide treatment

Male (**A**) and female (**B**) mice were weighed on alternate days for 2 days preceding gene induction and up to 4 weeks after placebo or glibenclamide pellet implantation (at day 2). Tamoxifen (Tx) was given at day 0 to induce gene expression. Results are mean for control mice (●, n=2 males and 2 females), and mean ± SEM for induced iβ-V59M mice implanted with placebo pellets (○, n=6 males and 6 females) and induced iβ-V59M mice implanted with glibenclamide pellets (●, n=9 males and 10 females). IPGTT = intraperitoneal glucose tolerance test; OGTT = oral glucose tolerance test.

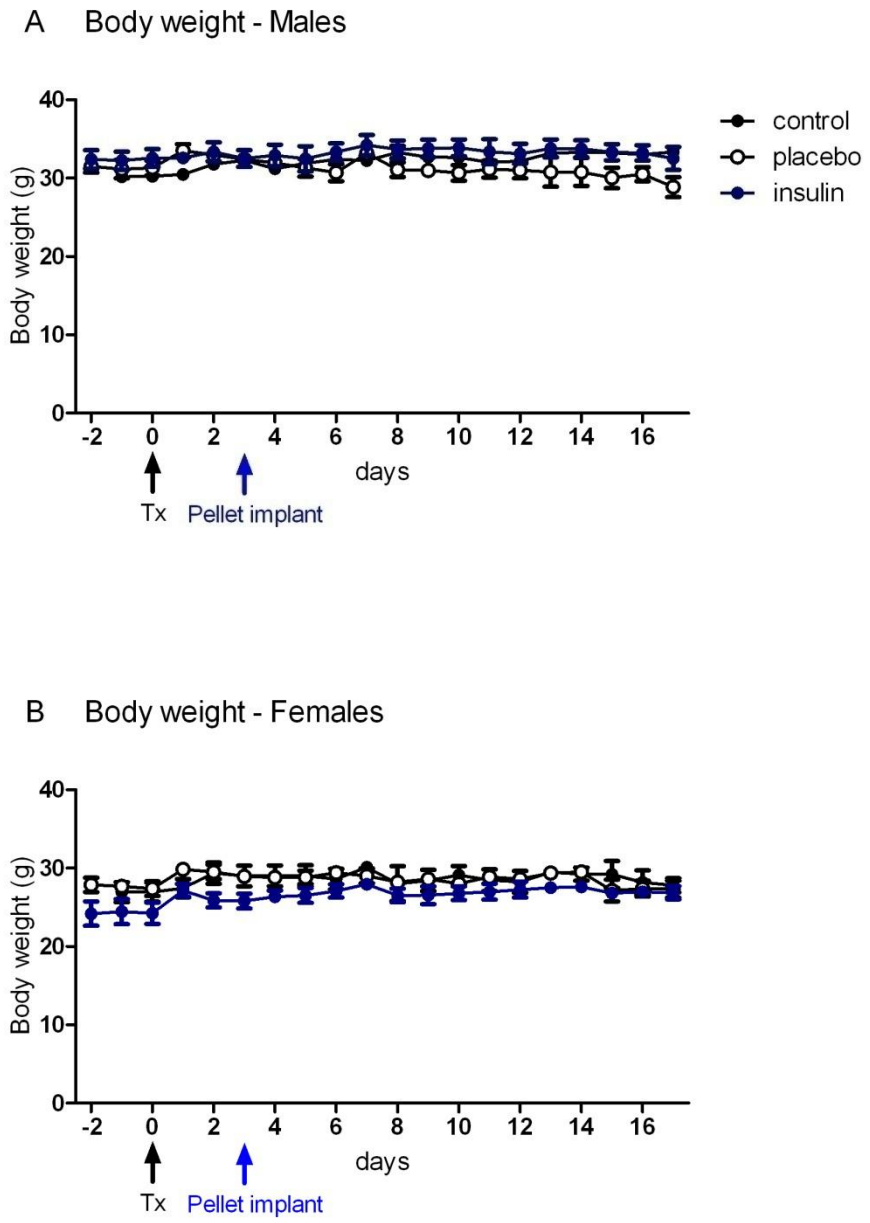


Figure 3.4: Body weight - insulin treatment

Male (**A**) and female (**B**) mice were weighed daily for 2 days preceding gene induction and up to 2 weeks after placebo or insulin pellet implantation (at day 3). Tamoxifen (Tx) was given at day 0 to induce gene expression. Results are mean ± SEM for control mice (●, n=6 males and 6 females), induced iβ-V59M mice implanted with placebo pellets (○, n=5 males and 6 females) and induced iβ-V59M mice implanted with insulin pellets (●, n=11 males and 11 females).

Interestingly, induced iβ-V59M male mice implanted with placebo pellets only lost a minor amount of body weight within the first 2 weeks after pellet implantation (Figure 3.4A). However, a major decrease in body weight (~30%) was observed 4 weeks after pellet implantation (Figure 3.3A). It is likely this is due to the severe diabetes they suffered from. By contrast, female induced iβ-V59M mice implanted with placebo pellets did not show a decrease in body weight despite suffering from diabetes.

3.1.4 Mice bred on a pure genetic background develop a more severe phenotype

All experiments were conducted using mice bred on either a pure C3H/HeJ or a mixed genetic background (C57Bl/6, C3H/HeJ, BALB/c). Following gene induction and placebo pellet implantation, iβ-V59M mice on a pure C3H/HeJ background developed slightly but significantly higher blood glucose levels. Four weeks after placebo pellet implantation, blood glucose levels averaged 27.5 ± 0.2mM (n=4), compared with 24.7 ± 0.4mM (n=11; $P<0.001$) measured for induced iβ-V59M mice on a mixed genetic background (Table 1). However, the FreeStyle Lite Blood Glucose Monitoring System only displayed blood glucose measurements ≤ 27.8mM. The majority of mice bred on a pure C3H developed higher blood glucose levels and therefore their diabetes might even be worse than displayed in Table 1.

The different genetic backgrounds had no effect on blood glucose levels measured in induced iβ-V59M mice implanted with insulin or glibenclamide pellets or in control mice (Table 1). No difference was found between data obtained from male and female mice so results were pooled in order to examine statistical significance of differences between the two genetic backgrounds.

Table 1: Average free–fed blood glucose levels for mice bred on a pure C3H/HeJ background vs a mixed genetic background

Treatment	Average free-fed blood glucose levels (mean ± SEM)		Statistical significance
	Pure genetic background	*Mixed genetic background*	*t-test*
Control	5.8 ± 0.1mM (n=6)	5.6 ± 0.1mM (n=18)	*ns*
Insulin	5.5 ± 0.1mM (n=2)	5.9 ± 0.6mM (n=20)	*ns*
Glibenclamide	5.9 ± 0.2mM (n=2)	5.5 ± 0.1mM (n=17)	*ns*
Placebo	27.5 ± 0.2mM (n=4)	24.7 ± 0.4mM (n=11)	*P<0.001*

Differences in body weight were also observed between the two genetic backgrounds. Mice bred on a pure C3H/HeJ genetic background (whether controls or induced iβ-V59M mice implanted with a glibenclamide pellet) gained up to 15% in body weight between 12 and 16 weeks of age, whereas the body weight of mice bred on a mixed genetic background increased only 4%. Placebo-treated induced iβ-V59M mice on a C3H/HeJ background showed a major decrease in body weight (up to 27%) after 4 weeks of diabetes, whereas no decrease in weight was seen on a mixed genetic background. No influence of genetic background on body weight was seen in induced iβ-V59M mice implanted with insulin pellets (Table 2).

Data obtained from male and female mice were pooled as they were similar but as only a limited number of mice bred on a pure C3H/HeJ background were available, no statistical analysis was possible.

Table 2: Body weight change after pellet implantation - pure C3H/HeJ background vs mixed genetic background

Treatment	Body weight change after pellet implantation (%)			
	Pure genetic background		*Mixed genetic background*	
Control				
After 2 weeks	+5%	(n=4)	-2%	(n=8)
After 4 weeks	+10%	(n=2)	+3%	(n=10)
Insulin				
After 2 weeks	+2%	(n=2)	+1%	(n=20)
Glibenclamide				
After 4 weeks	+15%	(n=2)	+4%	(n=17)
Placebo				
After 2 weeks	-7%	(n=1)	-5%	(n=10)
After 4 weeks	-27%	(n=3)	+9%	(n=1)

3.2 The effect of glibenclamide and insulin on glucose tolerance

As previously shown glibenclamide and insulin reversed the elevation of blood glucose produced by induction of Kir6.2-V59M expression to physiological levels. In order to determine if both agents also normalized the physiological response to administration of a glucose load, intraperitoneal (IPGTT) and oral (OGTT) glucose tolerance tests were carried out.

3.2.1 Glucose tolerance tests reveal a gender difference in response to glucose

An IPGTT and an OGTT were first performed on 12-week old control (ROSA and wild-type mice) and uninduced iβ-V59M mice. Blood glucose levels after a 16-18 hour fast were similar for all mice used in both tests (Figures 3.5A and B). Blood glucose concentrations rose to a maximum 30 minutes after glucose was given by either intraperitoneal injection (IPGTT), or by oral gavage (OGTT), and then decreased to fasting levels after 120 minutes. There was a significant difference between female control (n=12) and uninduced mice (n=21) in both, the IPGTT (*P<0.01*) and the OGTT (*P<0.05).* By contrast, male control (n=12) and uninduced mice (n=19) were not different. Blood glucose concentrations measured at 120 minutes after glucose administration were similar in control and uninduced mice. The reason for the difference between control and uninduced female mice at the 30 minute time point is unclear, but may be related to the fact that the line was maintained on a mixed genetic background (C57BL/6, C3H/HeJ, BALB/c).

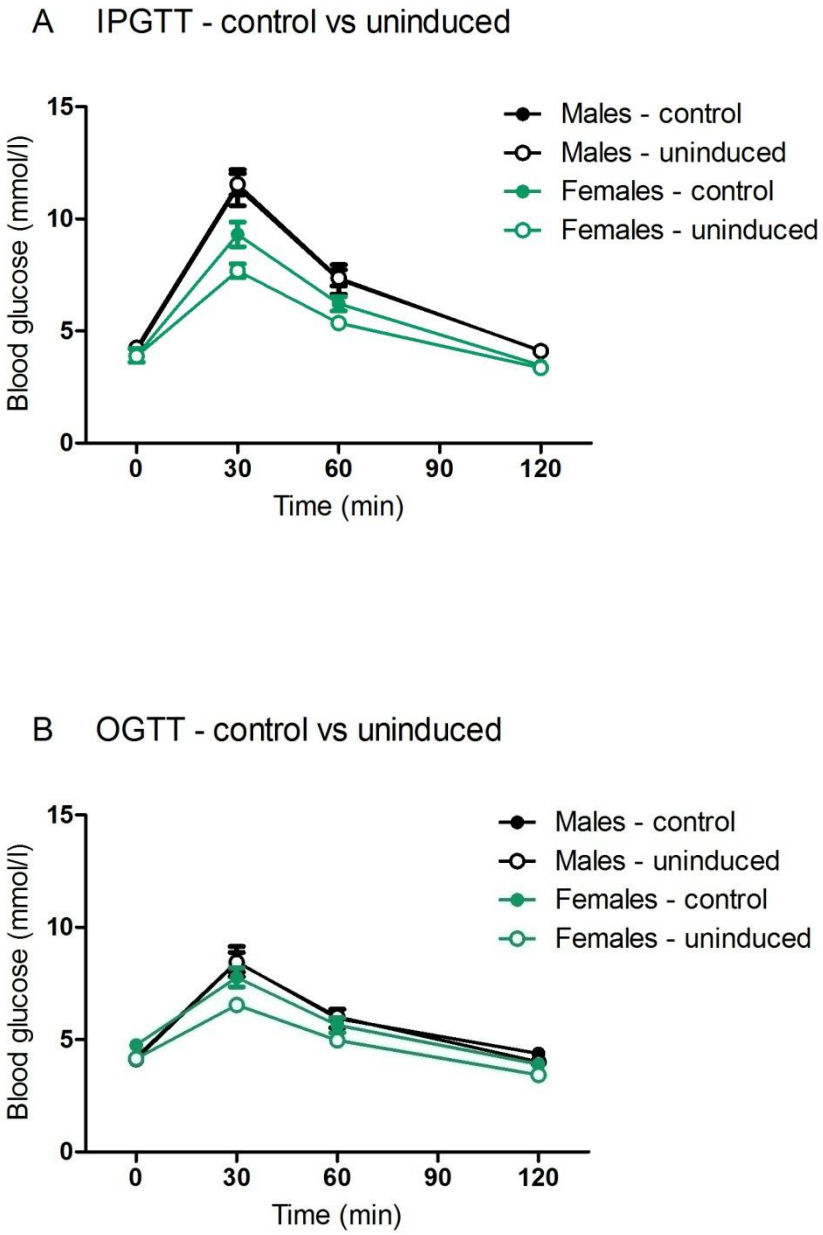


Figure 3.5: IPGTT and OGTT: control vs uninduced iβ-V59M mice

IPGTT (**A**) and OGTT (**B**) were performed on male (black line) and female (green line) mice. Results are mean ± SEM for control (●, n=12 males and 12 females) and uninduced iβ-V59M (○, n=26 males and 29 females) mice.

There was also a gender difference in the response to an IPGTT. Blood glucose levels of male and female control mice measured 30 minutes after glucose injection revealed a significant difference (*P<0.01*) (Figures 3.5A and B). Blood glucose concentrations of uninduced male and female iβ-V59M mice were even more significantly different and remained so for up to 60 minutes after glucose injection (*P<0.001*).

3.2.2 The response of untreated and treated diabetic mice to an IPGTT

An IPGTT was carried out on 12-week old male (n=26) and female (n=29) iβ-V59M mice both prior to gene induction and in the same mice after gene induction and one of 3 different treatments. Subcutaneous placebo pellets were administered to 10 male and 8 female mice and an IPGTT performed 2 weeks later. Subcutaneous insulin pellets were administered to 7 male and 8 female mice and an IPGTT performed 2 weeks later. A subcutaneous glibenclamide pellet was administered to 9 male and 10 female mice and an IPGTT performed both 2 and 4 weeks later. All data sets are plotted on the same graph to enable them to be more easily compared.

Figures 3.6A and B reveal that expression of Kir6.2-V59M had a dramatic effect on glucose tolerance. After 2 weeks of gene expression, fasting blood glucose levels were significantly elevated in placebo-treated induced iβ-V59M mice. After fasting for 16-18 hours, blood glucose was 7.5 ± 1.4mM (n=7 males) and 10.4 ± 1.9mM

(n=8 females) compared to 4.3 ± 0.1mM (n=26 males) and 3.9 ± 0.1mM (n=29 females) in animals tested prior to gene induction.

In response to a glucose load, blood glucose rose to 16.2 ± 2.1mM (n=7 males) and 20.2 ± 2.3mM (n=8 females) (Table 3) and remained elevated (>10mM) for 2 hours (Figures 3.6A and B). Figures 3.6A and B also show that male placebo-treated induced iβ-V59M mice responded better to an intraperitoneal glucose challenge than female mice.

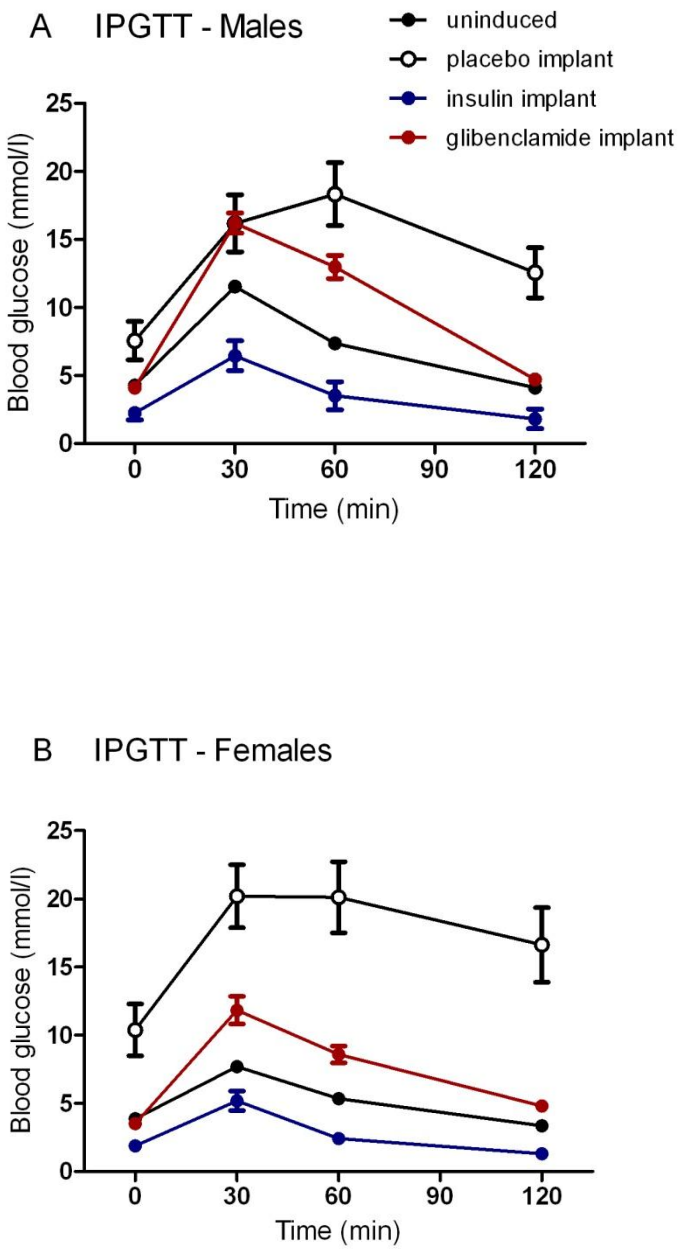


Figure 3.6: Intraperitoneal glucose tolerance test (IPGTT)

An IPGTT was performed on male (**A**) and female (**B**) induced iβ-V59M mice prior to gene induction (●, n=26 males and 29 females), 2 weeks after gene induction and insulin pellet implantation (●, n=10 males and 11 females); 2 weeks after gene induction and placebo pellet implantation (○, n=7 males and 8 females); both 2 and 4 weeks after gene induction and glibenclamide implantation in the same animals (●, n=9 males and 10 females). Results are presented as mean values ± SEM.

Table 3: Blood glucose level measured 30 minutes after glucose load (IPGTT)

Treatment	Blood glucose (mM) at t=30min (mean ± SEM)					
	Males		*ANOVA (uninduced vs treatment)*	*Females*		*ANOVA (uninduced vs treatment)*
Uninduced	11.5 ± 0.5	(n=26)		7.7 ± 0.3	(n=29)	
Insulin	6.6 ± 1.2	(n=10)	*P<0.01*	5.2 ± 0.8	(n=11)	*ns*
Glibenclamide	16.2 ± 0.9	(n=9)	*P<0.001*	11.8 ± 1.0	(n=10)	*P<0.001*
Placebo	16.2 ± 2.1	(n=10)	*P<0.01*	20.2 ± 2.3	(n=8)	*P<0.001*

Table 3: As no difference in blood glucose at t=30min during an IPGTT was seen in induced iβ-V59M mice after 2 and 4 weeks of glibenclamide therapy, data were pooled.

Fasting blood glucose levels in glibenclamide-treated mice were similar to those obtained in uninduced mice (Figures 3.6A and B). However, the response to a glucose load was not fully restored by glibenclamide treatment. Thirty minutes after a glucose load, blood glucose levels in male mice (16.2 ± 0.9mM; n=9) were similar to those in placebo-treated animals (16.2 ± 2.1mM; n=10) (Table 3). Some improvement was seen in female mice: 30min after glucose load their blood glucose levels averaged 11.8 ± 1.0mM (n=10), which is significantly better than placebo-treated mice (20.2 ± 2.3mM; n=8) but still higher than measured in uninduced mice (7.7 ± 0.3mM; n=29) (Table 3). Blood glucose in both male and female mice had returned to fasting levels within 2 hours after glucose load, whereas it remained high in placebo-treated animals (Figures 3.6A and B). In summary, glibenclamide-treated mice showed an impaired glucose tolerance with respect to control animals, but performed significantly better at later time-points than placebo-treated mice.

Induced iβ-V59M mice implanted with insulin pellets were only fasted for 4-5 hours, as a longer fasting period increased their risk of hypoglycaemia and even this short fast was sufficient to lower their blood glucose concentrations below that of uninduced mice (Figures 3.6A and B). Insulin-treated induced iβ-V59M mice also showed an even better response to glucose than uninduced mice. Blood glucose levels during an IPGTT were significantly lower at 30 and 60 minutes after a glucose load and even fell below fasting levels within 2 hours (Table 3; Figures 3.6A and B). In summary, in mice implanted with insulin pellets the glucose response was shifted to lower glucose levels than seen for uninduced animals, indicating improved glucose tolerance. Both, insulin and sulphonylurea therapy appeared to be more effective in female mice.

3.2.3 The response of untreated and treated diabetic mice to an OGTT

It is evident from Figures 3.5A and B that the glucose response to an OGTT in uninduced mice is much lower than that for an IPGTT in the same mice. This is particularly the case for male mice, where 30 minutes after a glucose load the blood glucose concentration was only 8.4 ±0.4mM (n=26) during an OGTT compared with 11.5 ± 0.5mM in an IPGTT (Table 4). Female mice showed the same trend but the difference was smaller (IPGTT: 7.7 ± 0.3 versus OGTT: 6.5 ± 0.3mM; n=29) (Table 5). This difference is thought to be mediated by incretins, released from the gut when glucose is given orally, which stimulate insulin secretion and thus reduce the rise in blood glucose levels [65, 88].

Table 4: Comparison between blood glucose levels 30 minutes after a glucose load in an OGTT and IPGTT in male mice

Treatment	Blood glucose (mM) at t=30min (mean ± SEM)			
	n	*IPGTT*	*OGTT*	*t-test*
Uninduced	26	11.5 ± 0.5	8.4 ± 0.4	*P<0.001*
Insulin	10	6.6 ± 1.2	8.4 ± 1.8	*ns*
Glibenclamide	9	16.2 ± 0.9	12.9 ± 0.8	*P<0.01*
Placebo	10	16.2 ± 2.1	21.9 ± 2.1	*ns*

Table 5: Comparison between blood glucose levels 30 minutes after a glucose load in an OGTT and IPGTT in female mice

Treatment	Blood glucose (mM) at t=30min (mean ± SEM)			
	n	*IPGTT*	*OGTT*	*t-test*
Uninduced	29	7.7 ± 0.3	6.5 ± 0.3	*P<0.01*
Insulin	11	5.2 ± 0.8	5.9 ± 0.6	*ns*
Glibenclamide	10	11.8 ± 1.0	11.8 ± 0.8	*ns*
Placebo	8	20.2 ± 2.3	22.4 ± 0.9	*ns*

The incretin effect is reduced in patients with type 2 diabetes [80] and ND patients treated with insulin [8]. However, when ND patients are treated with sulphonylureas, the incretin response is restored [8]. In order to examine if the same effect occurs in our mouse model, an OGTT was carried out in the same animals 3-4 days after an IPGTT. The results were similar in male and female mice (Figures 3.7A and B; Tables 4 and 5).

Prior to an OGTT, induced iβ-V59M mice that had received placebo treatment for 2 weeks, and which had thus been exposed to elevated blood glucose levels, were fasted for 16-18 hours. Their fasting glucose levels were almost 4-fold higher (~15mM vs 4mM) than those in the same animals prior to gene induction (Figures 3.7A and B) and significantly worse than seen with the earlier IPGTT. The reason for this is unclear. The OGTT was performed 1 week after the IPGTT: thus perhaps the worsening diabetes had impaired insulin secretion further.

Similarly, placebo-treated induced iβ-V59M mice showed higher blood glucose levels at 30 minutes after glucose was given by oral gavage than when given by intraperitoneal injection. In male mice (n=10) plasma glucose rose to 21.9 ± 2.1mM (OGTT) compared with 16.2 ± 2.1mM (IPGTT), and in females (n=8) to 22.4 ± 0.9mM (OGTT) compared to 20.2 ± 2.3mM (Tables 4-5). Placebo-treated animals were also far less glucose tolerant than controls (Figures 3.7A and B; Table 6). These results show that no incretin effect was detectable after 2 weeks of diabetes. The absence of an incretin effect was also reported in patients suffering from type 2 diabetes [80].

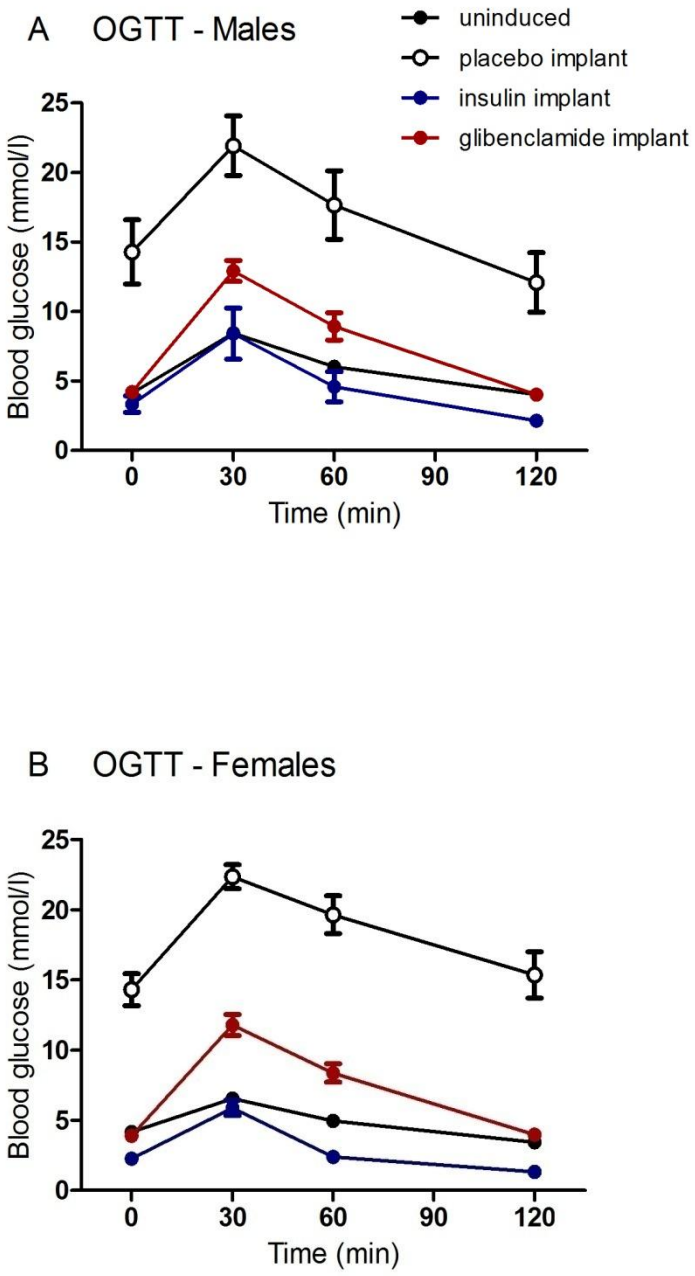


Figure 3.7: Oral glucose tolerance test (OGTT)

An OGTT was performed on male (**A**) and female (**B**) iβ-V59M mice prior to gene induction (●, n=26 males and 29 females), 2 weeks after gene induction and insulin pellet implantation (●, n=10 males and 11 females), 2 weeks after gene induction and placebo pellet implantation (○, n=7 males and 8 females) and 2 and 4 weeks after gene induction and glibenclamide implantation (●, n=9 males and 10 females). Results are presented as mean values ± SEM.

Table 6: Blood glucose levels 30 minutes after glucose load in an OGTT

Treatment	Blood glucose (mM) at t=30min (mean ± SEM)					
	Males		*ANOVA (uninduced vs treatment)*	*Females*		*ANOVA (uninduced vs treatment)*
Uninduced	8.4 ± 0.4	(n=26)		6.5 ± 0.3	(n=29)	
Insulin	8.4 ± 1.8	(n=10)	*ns*	5.9 ± 0.6	(n=11)	*ns*
Glibenclamide	12.9 ± 0.8	(n=9)	*P<0.001*	11.8 ± 0.8	(n=10)	*P<0.001*
Placebo	21.9 ± 2.1	(n=10)	*P<0.001*	24.4 ± 0.9	(n=8)	*P<0.001*

Insulin therapy fully normalized the response to an oral glucose load and glibenclamide substantially improved it (Figures 3.7A and B; Table 6). Interestingly, in contrast to placebo-treated animals, male mice (n=9) treated with glibenclamide showed better glucose tolerance at t=30min in an OGTT (12.9 ± 0.8mM) than in an IPGTT (16.2 ± 0.9mM) (Table 4). This suggests an improved incretin response in drug-treated mice. As expected, there was no difference in the response to an OGTT and IPGTT in insulin-treated animals (Table 4).

3.3 The effect of glibenclamide and insulin therapy on islet function and morphology

Previous studies have shown that, when the Kir6.2-V59M mutation is activated prior to birth, it leads to a severe decline in pancreatic islet function and changes in pancreas and islet morphology [82]. Unpublished studies by Kenju Shimomura indicate that a similar effect occurs when the gene is activated in adult life. A decrease in the number of insulin-containing β-cells per islet was observed which

might explain why pancreatic islets isolated from diabetic mice contained less insulin than healthy islets. This could contribute to the impaired insulin secretion and result in hypoinsulinemia [82, 89].

In order to determine whether these changes could be improved or even reversed by high-dose glibenclamide or insulin therapy, I compared insulin secretion, insulin content and islet morphology/histology from uninduced mice, and induced iβ-V59M mice that were subcutaneously implanted with either high-dose glibenclamide or insulin pellets.

3.3.1 Insulin secretion differs depending on therapy

Pancreatic islets were isolated from male and female control mice (ROSA, wild-type) and from induced iβ-V59M mice that had been treated with glibenclamide for 4 weeks or treated with insulin for 2 weeks. Islets were also isolated from mice that had received insulin-placebo pellets (for 2 weeks) or glibenclamide-placebo pellets (for 4 weeks).

Isolated islets were perifused with a 2mM glucose solution, followed by a 20mM glucose solution and subsequently by a 20mM glucose solution supplemented with 0.5mM tolbutamide. Tolbutamide, a sulphonylurea drug, was used to close the K_{ATP} channel and thereby stimulate insulin secretion. If there are no changes in islet composition, insulin content or drug efficacy, the tolbutamide response should be similar for wild-type and mutant islets because I used a maximally effective

concentration of tolbutamide (500µM) that should close almost all K_{ATP} channels [8].

Figures 3.8 A-B and 3.9 A-B show that basal insulin secretion (at 2mM glucose) was very low, and comparable in all islets tested. Elevation of the glucose concentration to 20mM triggered a 3 to 4-fold (males, n=4) and a 6 to 8-fold (females, n=4) increase in insulin secretion from control islets. Insulin secretion then gradually decreased until tolbutamide was added. This drug caused an additional boost in insulin secretion in all control islets. Islets isolated from glibenclamide-treated male (n=6) and female (n=5) mice failed to respond when the glucose concentration was raised from 2mM to 20mM (Figures 3.8A and B). However, tolbutamide produced a robust response.

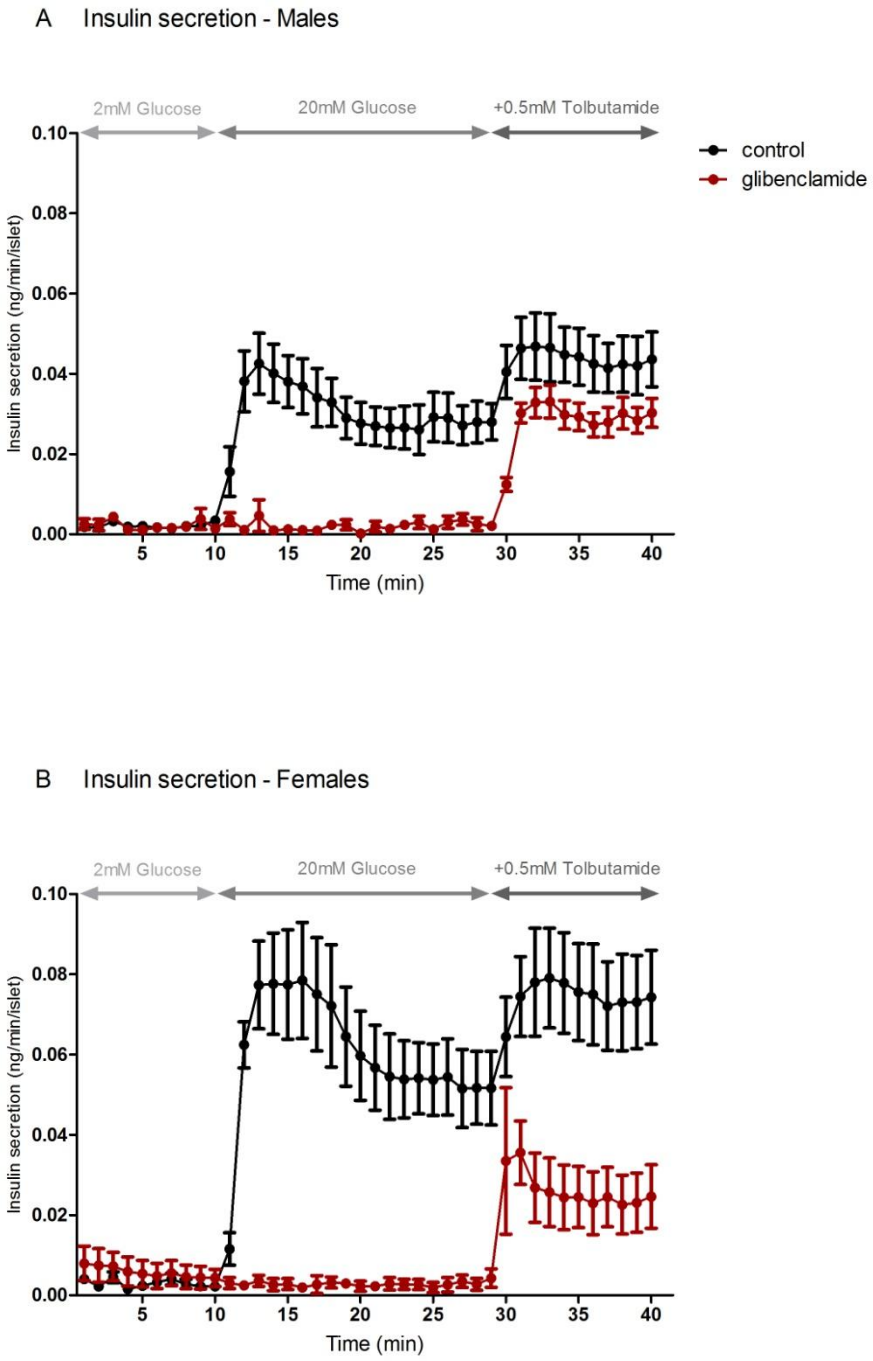


Figure 3.8: Insulin secretion: glibenclamide treated induced iβ-V59M mice

Insulin secretion from overnight cultured and subsequently perifused islets isolated from male (**A**) and female (**B**) mice in response to 2mM glucose, 20mM glucose, and to 20mM glucose + 0.5mM tolbutamide. Results are mean ± SEM for control mice (●, n=4 males and 4 females) and for induced iβ-V59M mice 4 weeks after glibenclamide implantation (●, n=6 males and 5 females).

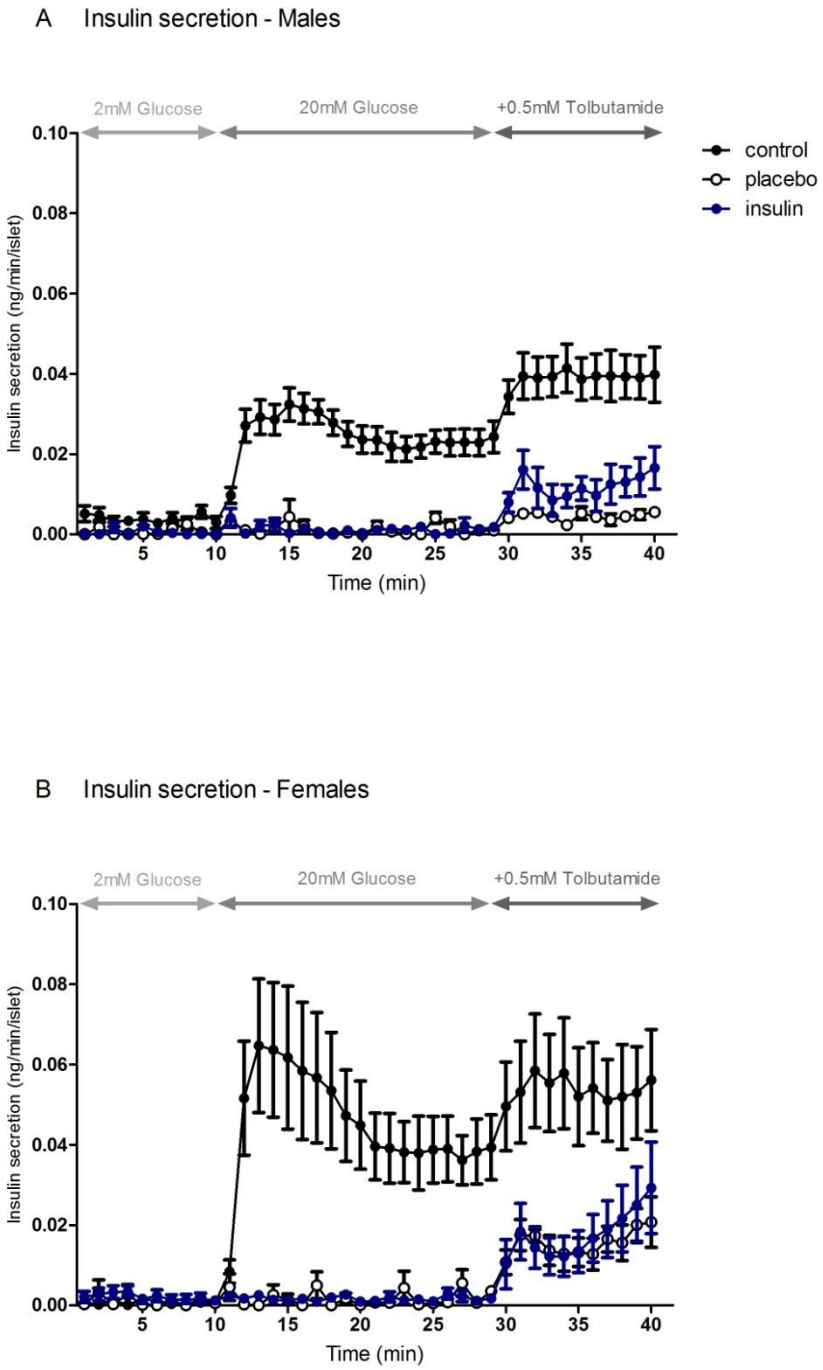


Figure 3.9: Insulin secretion: insulin treated induced iβ-V59M mice

Insulin secretion from overnight cultured and subsequently perifused islets isolated from male (**A**) and female (**B**) mice in response to 2mM glucose, 20mM glucose, and to 20mM glucose + 0.5mM tolbutamide. Results are mean ± SEM for control mice (●, n=4 males and 4 females) and for induced iβ-V59M mice 2 weeks after placebo implantation (○, n=3 males and 3 females) or insulin implantation (●, n=4 males and 5 females).

A similar effect was observed in islets isolated from insulin-treated (4 males and 5 females) mice, as well as from islets isolated from placebo-treated animals (Figures 3.9 A and B). In both cases, minimal insulin secretion was observed in response to glucose, but tolbutamide stimulated insulin secretion. There was no difference in the magnitude of the tolbutamide responses in female mice, but islets from male mice treated with placebo responded less well than those from male mice treated with insulin (Figures 3.8 A and B, 3.9A and B). Interestingly, islets from glibenclamide-treated animals responded noticeably better to tolbutamide (4-fold increase in insulin secretion) than those from insulin- or placebo-treated mice (1 to 2-fold increase in insulin secretion) (Figures 3.8 and 3.9).

3.3.2 Insulin treatment fails to preserve insulin content

All islets used for insulin secretion studies were lysed at the end of the experiment and their insulin content measured. Data obtained from male and female mice were plotted in separate graphs. As both genders displayed similar insulin content, data were also pooled and plotted together. Figure 3.10C reveals a trend for the insulin content in control mice to increase with age (between 14 and 16 weeks of age), but this is not significant. In contrast, the insulin content of male mice expressing the Kir6.2-V59M mutation decreased drastically (74%) when treated with placebo for 2 weeks. A smaller decrease was observed in female mice (37%) (Figures 3.10A and B). In both genders, glibenclamide therapy preserved the insulin content whereas insulin treatment was much less effective (Figures 3.10).

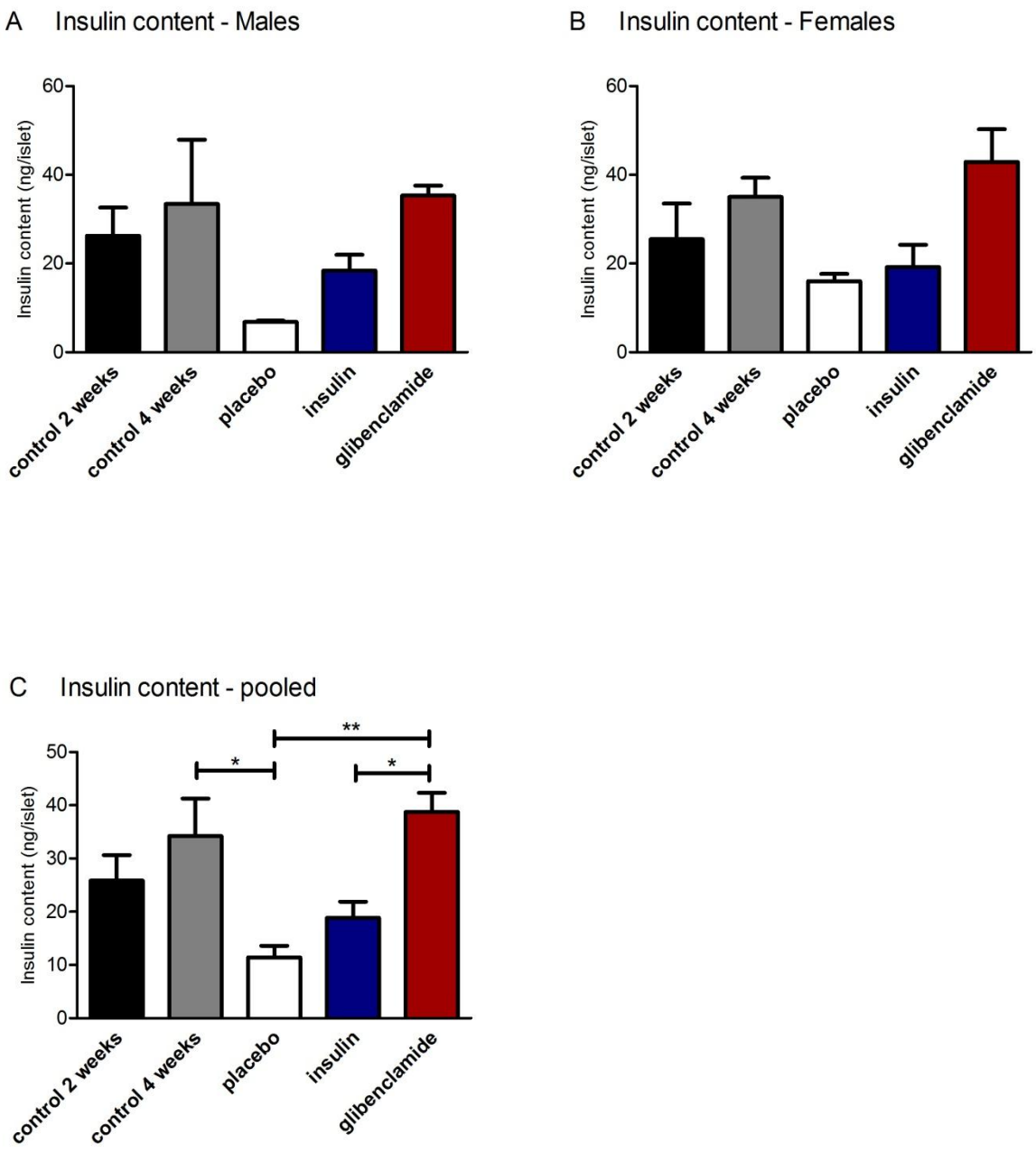


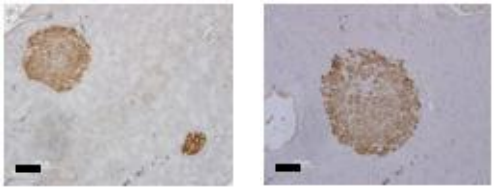
Figure 3.10: Insulin content

Insulin content measured in male (**A**) and female (**B**) pancreatic islets and pooled male and female data (**C**). Results are mean ± SEM for islets isolated from control mice 2 weeks (black bars, n=4 males and 4 females) and 4 weeks (grey bars, n=4 males and 4 females) after placebo pellet implantations, from induced iβ-V59M mice 2 weeks after placebo implantation (white bars, n=3 males and 3 females) or insulin implantation (blue bars, n=4 males and 5 females) and 4 weeks after glibenclamide implantation (red bars, n=6 males and 5 females). *P<0.05, **P<0.01.

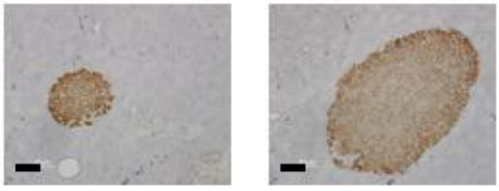
3.3.3 The effect of insulin and glibenclamide therapy on pancreatic islets

In order to examine the effect of insulin or sulphonylurea therapy on pancreatic islet morphology, size, number and β-cell area within each islet, slices of pancreas from male and female control mice and induced iβ-V59M mice implanted with placebo, insulin or glibenclamide pellets, were stained with an insulin antibody for histological analysis. Visual examination of all islets using light microscopy confirmed the characteristic well-defined and round shape of control islets, and that insulin-producing β-cells made up most of the islet (Figures 3.11A). Activation of Kir6.2-V59M gene expression and/or the associated elevation of blood glucose levels, led to a change in islet morphology: the majority of islets lost their round, clear shape and gradually became shapeless. Insulin-stained cells also decreased in number and showed intracellular vacuoles (Figures 3.11B). Two weeks of insulin therapy largely preserved islet shape but not the number of cells stained (Figures 3.11C). Interestingly, 4 weeks of glibenclamide treatment almost completely prevented the change in islet morphology and insulin staining (Figures 3.11D): visually there was no difference when comparing control and glibenclamide-treated islets, but there was a very dramatic difference when compared to islets from placebo-treated mice (Figures 3.11).

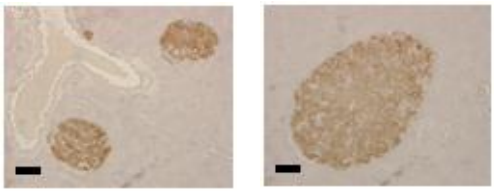
A



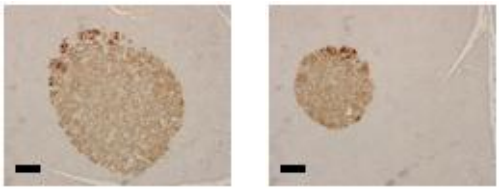
Control 2 weeks – Males



Control 2 weeks – Females

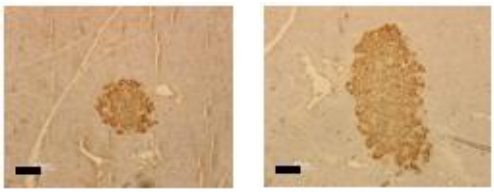


Control 4 weeks – Males

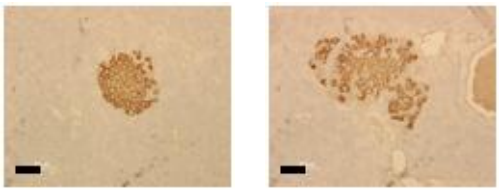


Control 4 weeks – Females

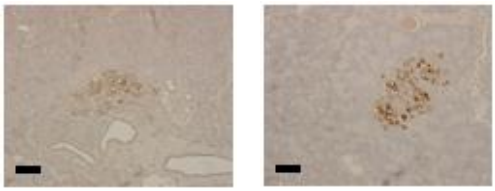
B



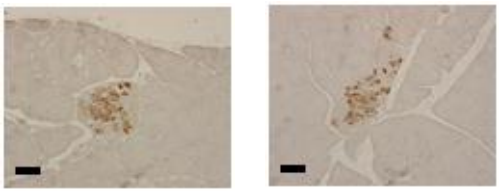
Placebo 2 weeks – Males



Placebo 2 weeks – Females



Placebo 4 weeks – Males



Placebo 4 weeks – Females

C



Insulin 2 weeks – Males

Insulin 2 weeks – Females

D



Glibenclamide 4 weeks – Males

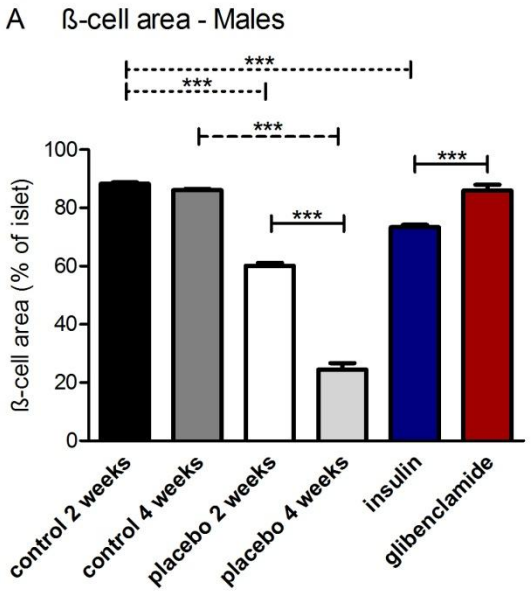
Glibenclamide 4 weeks – Females

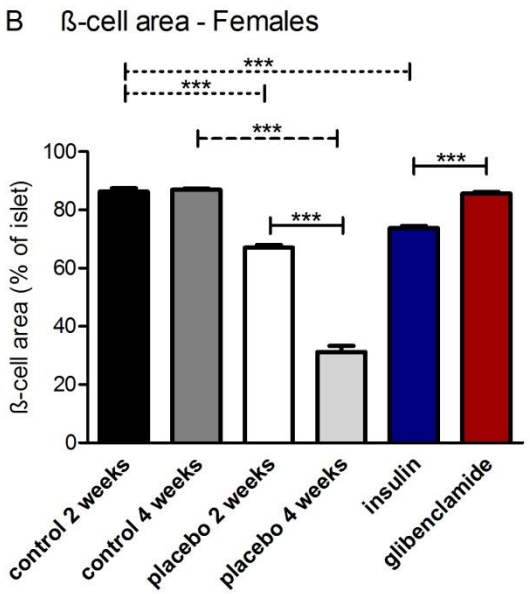
Figure 3.11: Insulin staining of mouse islets

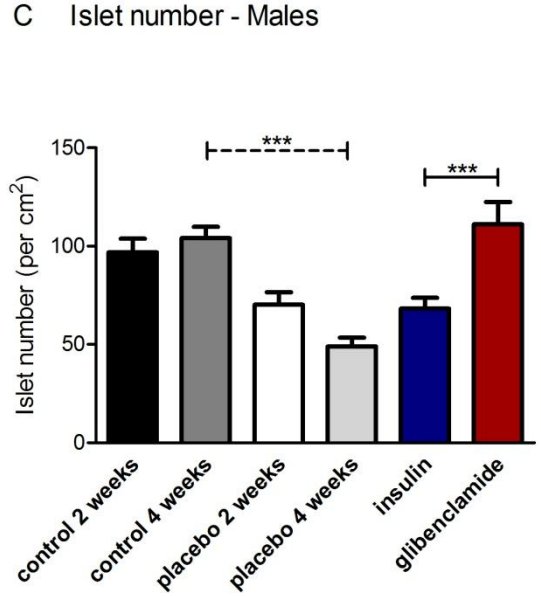
Sections of mouse pancreata were stained for insulin using DAB as the colour component which makes β-cells appear brown. Counterstaining followed with haematoxylin. Representative islets from male and female control islets 2 and 4 weeks after placebo pellet implantation (**A**). Representative islets from male and female islets from induced iβ-V59M mice 2 and 4 weeks after placebo pellet implantation (**B**). Representative islets from male and female islets from induced iβ-V59M mice 2 weeks after insulin pellet implantation (**C**). Representative islets from male and female islets from induced iβ-V59M mice 4 weeks after glibenclamide pellet implantation (**D**). Scale bar = 50µm (**A-D**).

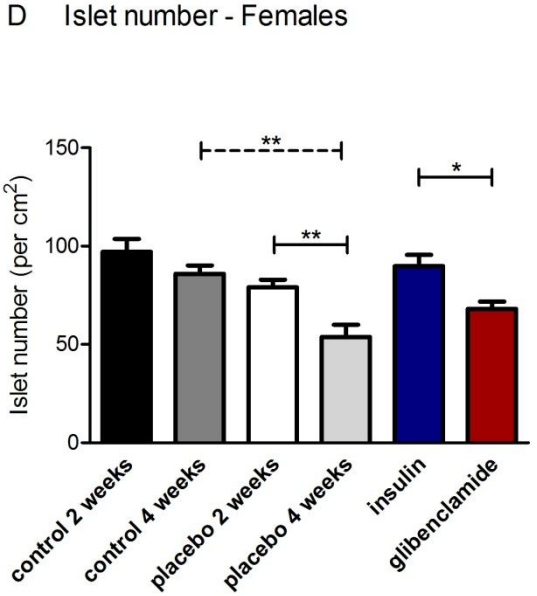
Girard *et al* (2009) [82] reported that the area of the islet occupied by insulin-staining β-cells in mice expressing the Kir6.2-V59M mutation from birth was 15-25% less than that found in islets from control mice (it decreased from ~85% to ~60%). When the gene was induced in adult life, similar results were obtained from male and female induced iβ-V59M mice that were kept hyperglycaemic for 2 weeks (placebo-treated) (Figure 3.12 A and B). Mice that were placebo-treated for 4 weeks showed an even more severe decrease in the % β-cell area/islet (55-60%). Interestingly, the % β-cell area in induced iβ-V59M mice treated with glibenclamide was no different to that of control mice. Insulin treatment reduced, but failed to completely prevent the deterioration in β-cell area (which was significantly smaller than that of control or glibenclamide-treated mice).

The number of islets per cm^2 of pancreas gradually decreased, with less than 50% remaining after 4 weeks of diabetes (gene induction) (Figures 3.12 C and D). In male mice, insulin failed to preserve the islet number, but glibenclamide prevented the decline in islet density. Interestingly, the opposite effect was seen in female mice.

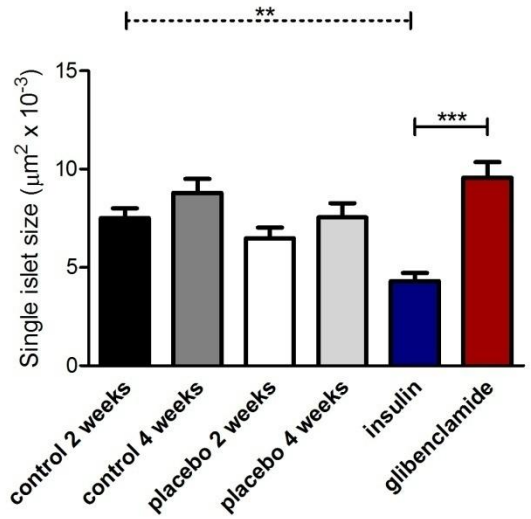

A ß-cell area - Males
ß-cell area (% of islet)
0
20
40
60
80
100
***
***
***
***
***
control 2 weeks
control 4 weeks
placebo 2 weeks
placebo 4 weeks
insulin
glibenclamide


B ß-cell area - Females
ß-cell area (% of islet)
0
20
40
60
80
100
***
***
***
***
***
control 2 weeks
control 4 weeks
placebo 2 weeks
placebo 4 weeks
insulin
glibenclamide

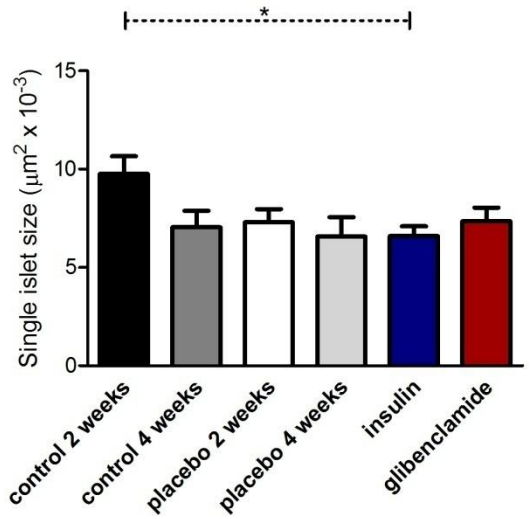

C Islet number - Males
Islet number (per cm2)
0
50
100
150
***
***
control 2 weeks
control 4 weeks
placebo 2 weeks
placebo 4 weeks
insulin
glibenclamide


D Islet number - Females
Islet number (per cm2)
0
50
100
150
**
**
*
control 2 weeks
control 4 weeks
placebo 2 weeks
placebo 4 weeks
insulin
glibenclamide

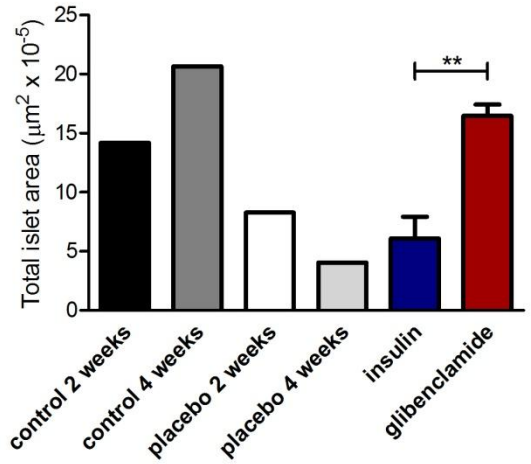
E Single islet size - Males



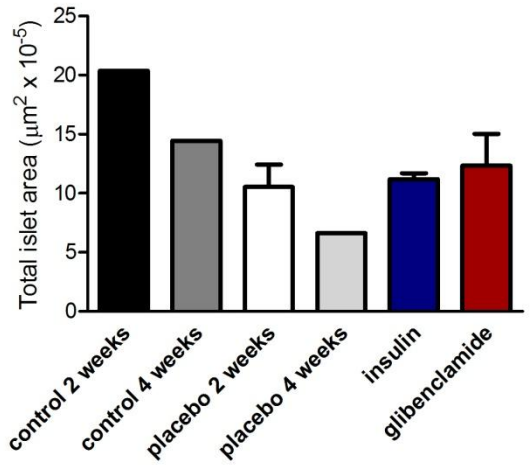
F Single islet size - Females



G Total islet area - Males



H Total islet area - Females



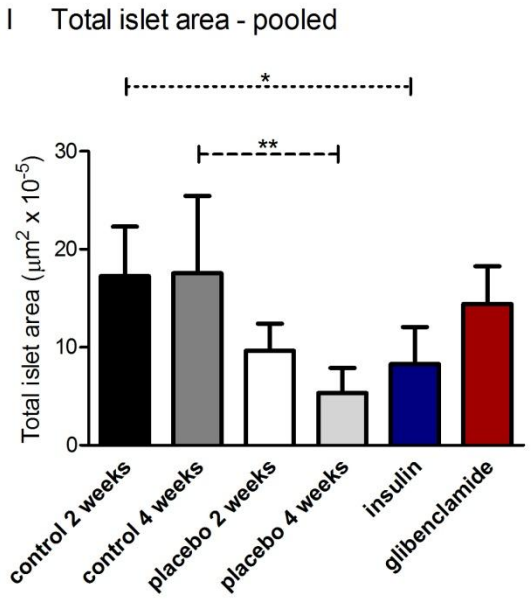


Figure 3.12: The effect of insulin and glibenclamide on islet morphology

Mean cross-sectional β-cell area expressed as the percentage of total islet cross-sectional area (**A**, **B**). Number of islets per cm^2 of pancreas (**C**, **D**). Mean single islet cross-sectional area (**E**, **F**). Mean total cross-sectional area (**G**, **H**). Mean total cross-sectional area (**I**, pooled). Results are mean ± SEM (5 sections per mouse) for control mice 2 weeks (black bars, n=2 males and 2 females, ~200 islets) and 4 weeks (dark grey bars, n=2 males and 2 females, ~210 islets) after placebo pellet implantations, induced iβ-V59M mice 2 weeks (white bars, n=2 males and 3 females, ~150islets) and 4 weeks (light grey bars, n=2 males and 2 females, ~170 islets) after placebo implantation, 2 weeks after insulin implantation (blue bars, n=4 males and 3 females, ~130 islets) and 4 weeks after glibenclamide implantation (red bars, n=3 males and 3 females, ~70islets). **P*<0.05, ***P*<0.01, ****P*<0.001.

Islet size was little affected by gene induction (diabetes) or by insulin or glibenclamide treatment (Figures 3.12 E and F). Oddly, there was a significant decline in islet size in male mice treated with insulin.

I also investigated if diabetes and insulin or glibenclamide therapy altered the total islet area within the pancreas. Statistical analysis was only possible to a limited extent because only 2 control mice and 2 diabetic mice were used for experiments lasting 2 or 4 weeks. Figures 3.12 G and H reveal that diabetes led to a loss of total islet area in 4 weeks of untreated hyperglycaemia. Glibenclamide therapy preserved the islet area in male mice. However, when diabetes was treated with insulin the total islet area significantly decreased. In female mice both drugs had no obvious effect on the total islet area. As control mice and placebo-, insulin- and glibenclamide-treated induced iβ-V59M show the same trend in total islet area, I plotted male and female data together (Figure 3.12I). The observations previously made for male and female mice were confirmed when pooled data were compared.

3.4 Insulin secretion: in vitro static incubation

The majority of patients suffering from neonatal diabetes are currently treated with glibenclamide. The average dose given is 0.45 mg/kg/day (range: 0.05 to 1.5 mg/kg/day) [8]. In order to determine which dose of glibenclamide triggers maximum insulin secretion in our mouse model, I measured insulin secretion using

batch incubations from wild-type mice and iβ-V59M mice after gene induction and elevation of free-fed blood glucose to more than 20mM.

3.4.1 Dimethyl sulfoxide (DMSO) does not decrease insulin secretion

Pancreatic islets from 14-week old male (n=6) and female (n=6) wild-type mice were incubated in solutions containing 2mM, 5mM, 10mM or 20mM glucose in the presence or absence of glibenclamide (20nM, 2µM or 20µM).

As glibenclamide was dissolved in DMSO (stock solution: 20mM glibenclamide), I first examined the effect of DMSO (0.1%) itself on insulin secretion. Data obtained from male and female mice were not significantly different and they were therefore put together. There was no difference in insulin secretion (Figure 3.13A) or insulin content (Figure 3.13B) in the presence of DMSO, which shows that the maximal concentration of DMSO used in these experiments did not affect insulin secretion. Figure 3.13A also shows that elevation of glucose from a basal level of 2mM to 20mM causes a 4-fold increase in insulin secretion.

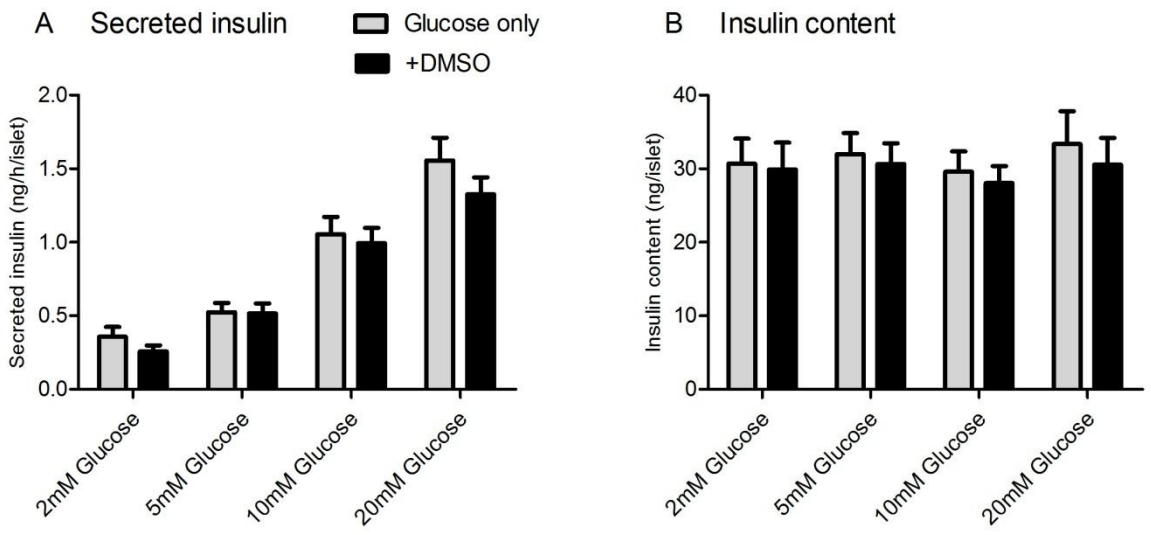


Figure 3.13: The effect of DMSO on insulin secretion and insulin content

Secreted insulin (**A**) and insulin content (**B**) from wild-type islets (n=12) were measured. Islets were incubated in 2mM, 5mM, 10mM or 20mM glucose with (black bars) or without (grey bars) DMSO. Results from male (n=6) and female (n=6) mice were pooled and data was plotted as mean ± SEM.

3.4.2 Glibenclamide initiates more insulin secretion in induced iβ-V59M mice

Insulin secretion was next measured from islets isolated from wild-type male (n=6) and female mice (n=6). The effect of glibenclamide (20nM, 2µM or 20µM glibenclamide) was examined on basal secretion at 2mM glucose, and in the presence of 5mM, 10mM and 10mM glucose. Glibenclamide only enhanced insulin secretion in 2mM and 5mM glucose solutions (Figures 3.14 A-D). Therefore, the effect of glibenclamide on insulin secretion from induced iβ-V59M mice was only measured in these glucose solutions. Presumably the lack of effect of

glibenclamide at higher glucose concentrations is because secretion is already maximally activated by glucose.

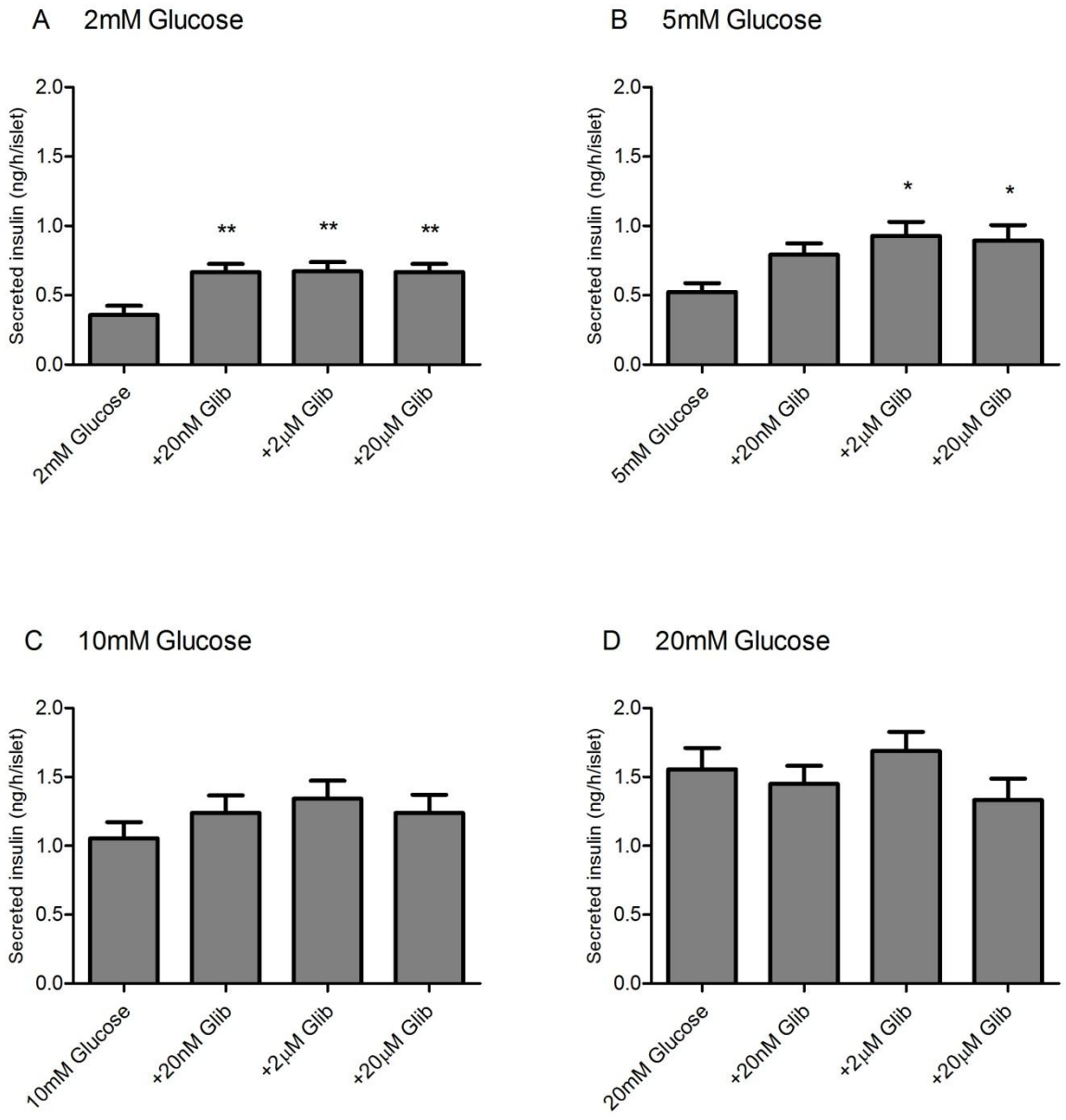


Figure 3.14: Insulin secretion from islets isolated from wild-type mice

Islets from wild-type mice (n=12) were incubated in 2mM (**A**), 5mM (**B**), 10mM (**C**) or 20mM (**D**) glucose with or without increasing concentrations of glibenclamide (20nM, 2μM or 20μM). Results from male (n=6) and female (n=6) mice were pooled and data was plotted as mean ± SEM. **P*<0.05, ***P*<0.01.

Kir6.2-V59M expression was induced in male (n=7) and female (n=7) iβ-V59M mice by tamoxifen injection at 14 weeks of age and islets were isolated one day after the blood glucose had risen above 20mM. They were then incubated in 2mM or 5mM glucose solutions alone or supplemented with glibenclamide (20nM, 2µM or 20µM). Data collected from male and female mice were not different and they were therefore pooled. Insulin secretion from pancreatic islets of wild-type mice and from mice in which Kir6.2-V59M expression had been induced was highest when incubated in glucose solutions containing 2µM glibenclamide. Compared to wild-type islets, islets from mice expressing the Kir6.2-V59M mutation secreted less insulin in basal (2mM) and 5mM glucose solutions. They were also not responsive to 20nM glibenclamide and needed a higher concentration of the drug (2µM) to stimulate insulin secretion (Figure 3.15A and B).

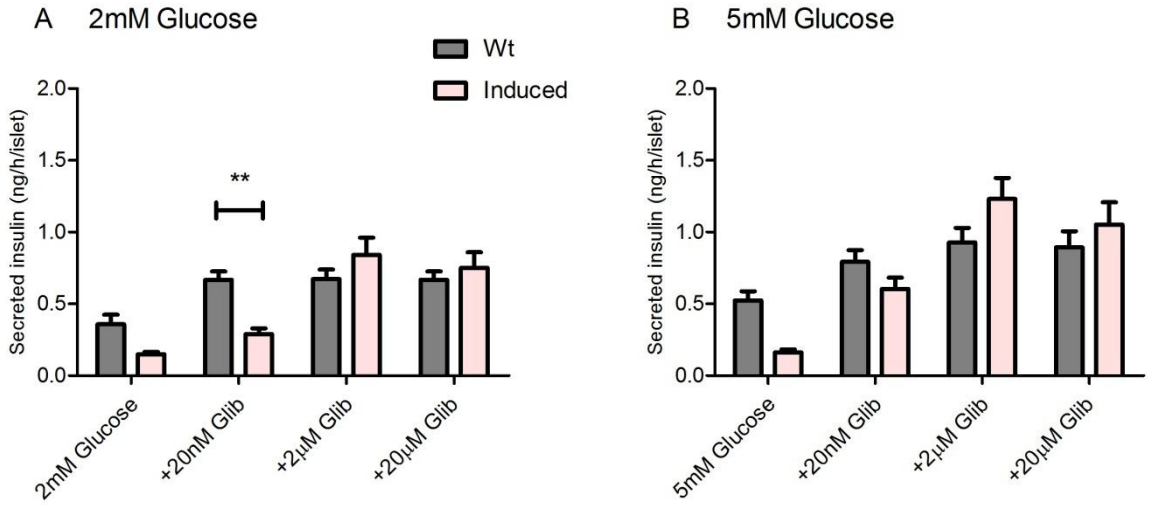


Figure 3.15: Insulin secretion: wild-type vs induced iβ-V59M mice

Islets from wild-type (grey bars, n=6 males and 6 females) and induced iβ-V59M (pink bars, n=7 males and 7 females) mice were incubated in 2mM (**A**) or 5mM (**B**) glucose with or without different glibenclamide concentrations (20nM, 2μM or 20μM). Results from male and female mice were pooled and plotted as mean ± SEM. ***P*<0.01.

3.4.3 Insulin content is not altered in induced iβ-V59M mice

Previous studies have shown that pancreatic islets isolated from untreated mice carrying a Kir6.2-V59M mutation from birth have a significantly lower insulin content compared to wild-type mice [82, 89]. In order to explore if insulin content is reduced immediately after Kir6.2-V59M gene expression, islets taken from wild-type mice and from iβ-V59M mice 3-4 days after tamoxifen injection were assayed for insulin content. No difference in islet insulin content between wild-type and induced mice was seen for islets in different glucose solutions (2mM, 5mM, 10mM or 20mM) either with or without glibenclamide supplementation (20nM, 2μM or

20µM). Islets from induced iβ-V59M mice contained a similar amount of insulin (Figure 3.16 A-D).

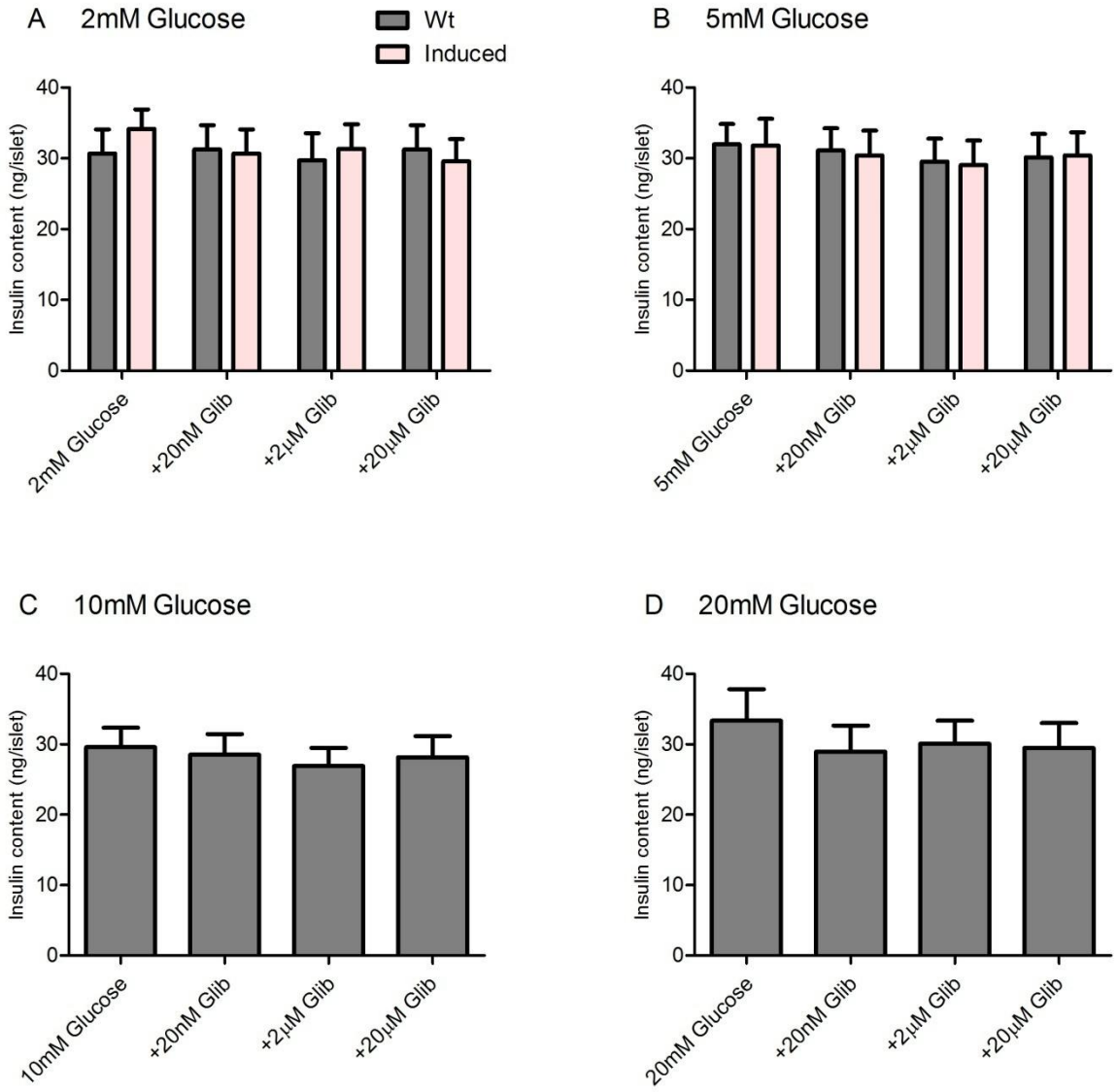


Figure 3.16: Insulin content: wild-type vs induced iβ-V59M mice

Islets from wild-type (grey bars, n=6 males and 6 females) and induced (pink bars, n=7 males and 7 females) mice were incubated in 2mM (**A**), 5mM (**B**), 10mM (**C**) or 20mM (**D**) glucose with or without different glibenclamide concentrations (20nM, 2µM or 20µM). Results from male and female mice were pooled and data was plotted as mean ± SEM.

3.5 The effect of glibenclamide on body weight and blood glucose in wild-type mice

3.5.1 Glibenclamide therapy does not cause a decrease in body weight

The drug glibenclamide is widely used as an anti-diabetic medication for patients suffering from type 2 diabetes mellitus or neonatal diabetes. Various trials on type 2 diabetes mellitus patients treated with glibenclamide have shown an increase in body weight [83, 84]. By contrast, anecdotal evidence seems to suggest that glibenclamide-treated neonatal diabetes patients lose body weight. To investigate what underlies this change in body weight, 12-week old wild-type mice were implanted with a placebo pellet (control, n=10) or a glibenclamide (2.5mg) pellet (treated, n=9). Body weight, food intake and water intake were monitored before and after pellet implantation. Both, control and drug-treated mice, showed a significant increase in body weight after pellet implantation ($P<0.05$, Figure 3.17A). This might suggest that mice that age are still growing. There was no difference in food or water intake between control and treated mice before and after pellet implantation (Figures 3.17B and C).

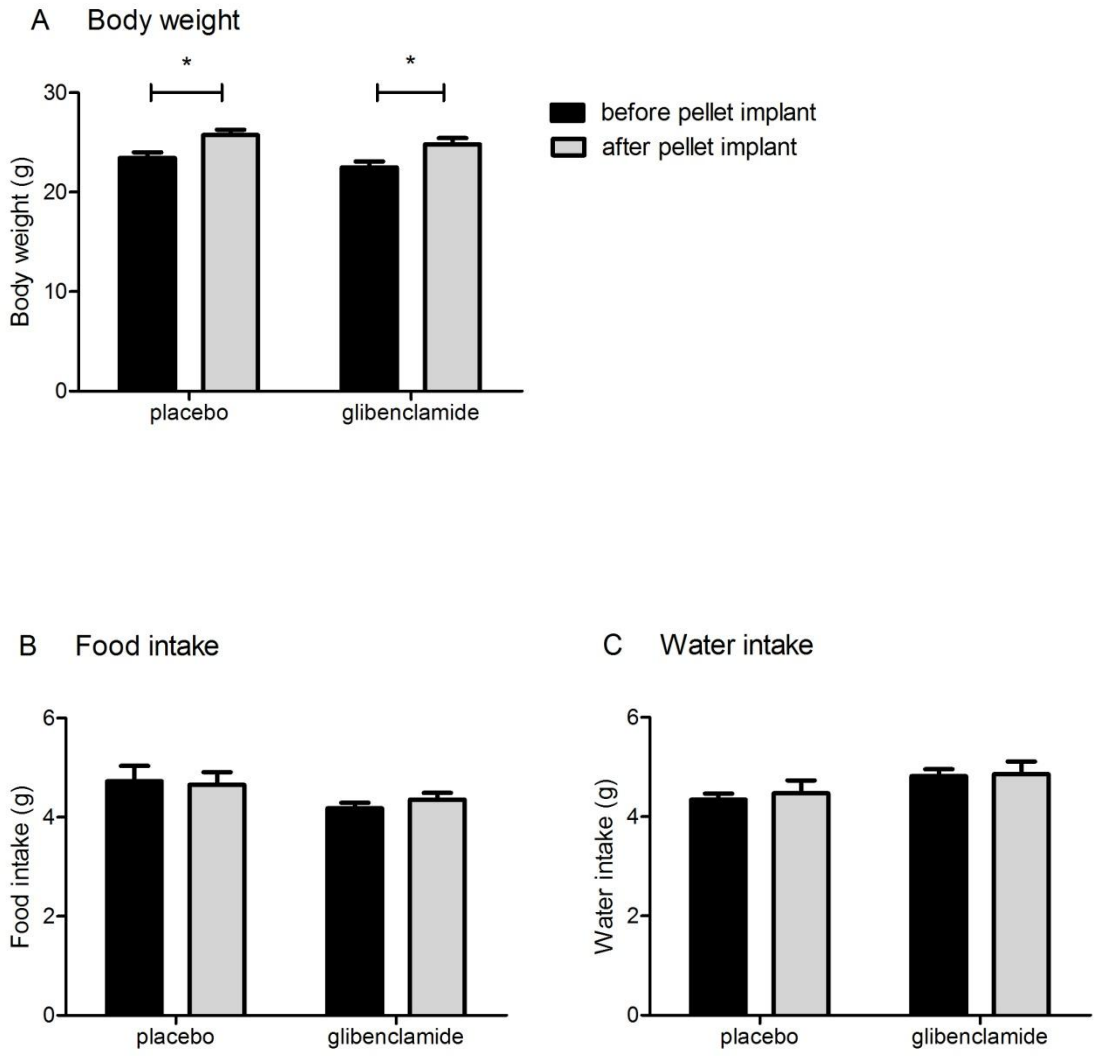


Figure 3.17: Body weight, food intake and water intake

Body weight (**A**), food intake (**B**) and water intake (**C**) of wild-type mice averaged over 4 weeks before and 4 weeks after placebo (n=10) or glibenclamide (n=9) pellet implantation. Results are mean ± SEM before (black bars) and after (grey bars) pellet implantation. *P<0.05.

3.5.2 Blood glucose is increased after glibenclamide therapy

Glibenclamide binds to the sulphonylurea receptor (SUR1) and directly closes the pancreatic K_{ATP} channel, leading to insulin release [66]. Therefore, one would expect that the blood glucose levels in wild-type mice treated with glibenclamide should be lower than that in mice implanted with placebo. However, glibenclamide treatment led to a significant *increase* in blood sugar levels (Figure 3.18). Similar findings have been reported previously, as discussed below.

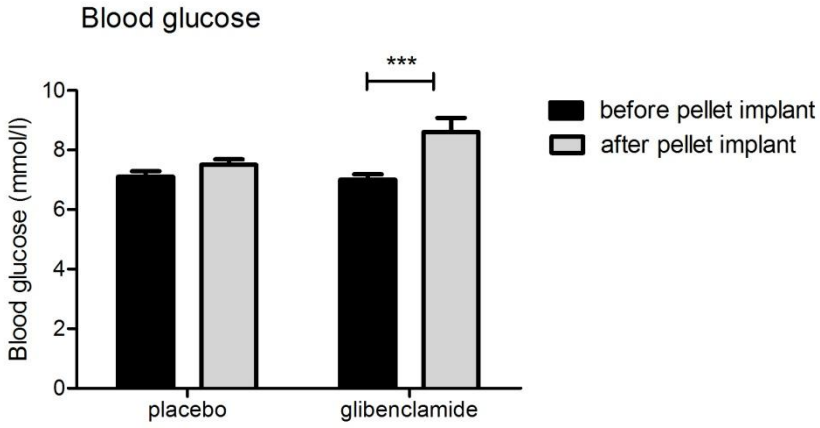


Figure 3.18: Blood glucose

Free-fed blood sugar levels of wild-type mice averaged over 4 weeks before and 4 weeks after placebo (n=10) or glibenclamide (n=9) pellet implantation. Results are mean ± SEM before (black bars) and after (grey bars) pellet implantation. ****P*<0.001.

Chapter 4: Discussion

4.1 The iβ-V59M mouse model: expression of neonatal diabetes in adulthood

Both, constitutive and inducible mouse models of neonatal diabetes have been used previously to examine the effect of gain-of-function K_{ATP} channel mutations [82, 89, 90]. Here, I concentrated on an inducible mouse model carrying the Kir6.2-V59M mutation in pancreatic β-cells. Gene expression was induced by tamoxifen in adulthood (induced iβ-V59M mouse): this allowed the investigation of drug therapy immediately after diabetes onset which is not possible in neonatal mice for technical reasons.

4.1.1 The Kir6.2-V59M mutation in pancreatic β-cells causes severe diabetes

Iβ-V59M mice developed severe diabetes 2-3 days after tamoxifen injection (Figures 3.1, 3.2) which showed that the activation of the Kir6.2-V59M mutation in pancreatic β-cells was sufficient to cause diabetes. Mice bred on a pure C3H/HeJ genetic background developed a more severe phenotype than mice bred on a mixed (C57Bl/6, C3H/HeJ, BALB/c) background: hyperglycaemia occurred 1-2 days after gene induction and blood glucose levels were significantly higher (Table 1). In addition, 4 weeks of diabetes led to a major decrease in body weight (~30%). In contrast, no loss of weight was observed in diabetic mice bred on a

mixed genetic background (Table 2). This might suggest that a clean genetic background leads to accelerated expression of mutant K_{ATP} channels in the pancreas, or that modifier genes are present in the mice of mixed genetic backgrounds that partially ameliorate the effects of K_{ATP} channel overactivity.

4.1.2 The effect of diabetes on pancreatic islets

Continual diabetes over 4 weeks had a major impact on the morphology and physiological function of pancreatic islets. Similar findings were reported by Girard *et al.* for a mouse model in which the Kir6.2-V59M gene was expressed selectively in pancreatic beta-cells prior to birth [82] and for mice with a different activating K_{ATP} channel mutation expressed selectively in beta-cells [89, 90].

The number of β-cells present within pancreatic islets decreased by at least 50% (Figures 3.12 A and B). The same trend was observed for the islet number and total islet area found in the pancreas (Figures 3.12 C-D, G-I). The round, well-defined islet shape also changed and islets appeared rough. Considerably less insulin-stained cells were found and they seemed to contain vacuoles, which may have harmed their function. Interestingly, islet size was not affected by diabetes (Figures 3.12 E and F).

This change in islet number and morphology might contribute to the lower efficacy of the sulphonylurea tolbutamide at stimulating insulin secretion (Figures 3.9A and B). Sulphonylurea drugs are known to bind to the SUR subunit of the K_{ATP} channel

which leads to channel closure and insulin secretion [66]. The marked reduction in insulin content will also contribute to the lower insulin secretion and may result in hypoinsulinemia [82, 89]. Previous studies have shown that very high extracellular glucose can impair insulin gene expression both in vivo and in vitro [82, 91]. I presume this is also the case in induced iβ-V59M mice as insulin staining was less intense in islets from diabetic mice.

Remedi *et al.* (2009) conducted similar experiments in an inducible mouse model of enhanced K_{ATP} channel activity combining an ATP-binding site mutation (K185Q) with an allosteric gating mutation (truncation of the N-terminal 30 amino acids, ΔN30) [89]. Gene induction resulted in a comparable phenotype to that seen in the iβ-V59M mouse model: progressively severe diabetes, profound loss of pancreatic β-cells and a dramatic reduction in insulin content. They also showed that progressive diabetes led to β-cell loss, increased α-cell number and α-cell infiltration within the islet (as visualized by glucagon staining). Staining for α-cells in severely diabetic iβ-V59M mice revealed the same trend (data not shown). This loss of insulin-staining might be caused by β-cell death and α-cell proliferation which has been reported previously [92-94], or by conversion of β-cells into α-cells (transdifferentiation) [95, 96], or simply by a decrease in insulin expression and a concomitant increase in glucagon expression in β-cells.

4.1.3 Glucose tolerance is severely impaired

Overnight fasting lowered blood glucose levels in induced iβ-V59M mice but they still remained well above those measured in control mice (~5mM) (Figures 3.6). Interestingly, an additional overnight fast 3-4 days later failed to bring blood glucose down below 15mM (Figures 3.7). The difference in fasting blood glucose might be due to more expression of mutant K_{ATP} channels in pancreatic islets or a further decrease in β-cell mass. The difference in fasting blood glucose levels seen with time might be worth exploring further.

Glucose tolerance was severely impaired (Figures 3.6, 3.7) and no enhancing effect of incretins on insulin secretion was detected when glucose was given orally (Tables 4, 5). This is explained by the fact that the stimulating effect of incretins is only enabled when K_{ATP} channels are shut because they are only effective when intracellular calcium is elevated, which is caused by membrane depolarization [65, 88].

4.1.4 Male iβ-V59M mice develop severe symptoms caused by diabetes

Severe diabetes for up to 4 weeks revealed a gender difference in general health, body weight, insulin secretion and insulin content (Figures 3.3, 3.4, 3.9 and 3.10). When compared to female induced iβ-V59M mice, the general health of male mice was worse. They deteriorated rapidly within 4 weeks after diabetes was induced and were in constant danger of dehydration as they urinated excessively. Male

diabetic mice also lost ~30% of body weight, whereas the body weight of female mice was similar to control mice. They also showed a more prominent decrease in insulin content that consequently led to severely impaired insulin secretion that could only be slightly enhanced by tolbutamide. Surprisingly, female diabetic mice were more glucose intolerant when injected with a glucose load. These observations confirm that overall, female mice are less affected by the disease than male mice. Perhaps oestrogen has a protective effect in diabetes [97].

4.2 Insulin – diabetes treatment without affecting the K_{ATP} channel

Insulin is a hormone that is secreted by pancreatic β-cells when blood glucose concentrations are elevated [98]. By binding to specific receptors, that are present on many cells, insulin stimulates glucose uptake and so restores the blood glucose concentrations to physiological levels.

4.2.1 Insulin therapy normalizes blood glucose concentrations and does not affect body weight

Insulin reversed the elevation in blood glucose levels produced by expression of the Kir6.2-V59M gene within 2 days after treatment was initiated (Figures 3.2). However, the hormone failed to stabilize blood glucose levels within the narrow range seen in control mice. Furthermore, in a few experiments when blood glucose was measured at different time points during the day striking fluctuations

were revealed, reaching from hypoglycaemia to hyperglycaemia, presumably reflecting changes in food intake.

Body weight in induced iβ-V59M mice treated with insulin was not altered (Figures 3.4). In contrast, insulin therapy in type 2 diabetes mellitus patients leads to an increase in body weight [87]. There are a number of possible explanations for this difference: firstly, type 2 diabetes and neonatal diabetes may be different - although there is no quantitative data, anecdotal evidence suggests most neonatal diabetes patients are not obese even when insulin treated; secondly, metabolic effects in mice and humans may be different; thirdly, weight gain may have been observed if induced iβ-V59M mice were treated for longer than 2 weeks with insulin.

4.2.2 The effect of insulin therapy on the pancreatic islet

Insulin treatment for 2 weeks failed to preserve β-cell area, islet number, single islet size and total islet area in male induced iβ-V59M mice. In female induced iβ-V59M mice, islet number was preserved but there was still a decrease in β-cell area, single islet size and total islet area (although not as much as in male mice) (Figures 3.11). In both, male and female mice, the majority of pancreatic islets kept their round and well-defined shape, but the amount of insulin-stained β-cells was less than in control mice (consistent with the lower insulin content). There was no difference between any of the morphometric parameters in islets from mice treated with insulin and mice treated with placebo pellets for 2 weeks: thus

although insulin maintains blood glucose levels it does not preserve beta-cell mass and morphology.

The reduction in islet insulin staining and the reduced β-cell area may explain the decrease in insulin content (Figures 3.10). It might also explain why insulin secretion from isolated islets was impaired after 2 weeks of insulin therapy and only showed little stimulation by tolbutamide. Islets from male mice showed slightly less insulin secretion than female mice and their insulin content was lower. This gender difference may be the reason why male induced iβ-V59M mice had higher blood glucose levels and urinated more profusely than female mice.

Previous studies have shown that hyperglycaemia impaired insulin gene expression [82, 91] as well as causing β-cell hyper-secretion [92]. Marshak *et al* (1999) [91] also suggested that this hyper-secretion was responsible for the imbalance between insulin synthesis and secretion and therefore led to the reduction in insulin content. Subsequently, restored blood glucose concentrations were shown to improve insulin gene expression, insulin content and insulin secretion. These findings also suggest that the small increase in insulin content and secretion seen in male insulin-treated mice could be correlated with more insulin gene expression. However, this would need to be confirmed by doing microarrays or quantitative real-time PCR.

Free-fed blood glucose levels were controlled in insulin-treated mice, and they showed normal glucose tolerance in both IPGTT and OGTT (Figures 3.6, 3.7),

implying that reduced insulin content and the morphological changes seen in insulin-treated mice are a consequence of K_{ATP} channel activation rather than insulin or plasma glucose levels. My data thus indicate that insulin therapy fails to prevent the deterioration of the number and function of pancreatic β-cells and islets. This suggests that it is not only necessary to maintain blood glucose levels, but also essential to close the mutant K_{ATP} channels in order to preserve pancreatic islets.

4.2.3 Insulin therapy and glucose tolerance

As insulin is constantly released from the pellets into the bloodstream even a short 4-5 hour fast resulted in blood glucose levels below control levels. Mice that were fasted overnight were in danger of suffering from severe hypoglycaemia.

The response to glucose was comparable to control mice but shifted to lower glucose levels which again might be due to the amount of insulin released from the pellets (Figures 3.6, 3.7). As expected, no stimulating effect of incretins was detectable in response to oral glucose when mice were treated with insulin (Tables 4, 5). This is because K_{ATP} channels remain open in the pancreatic β-cells of insulin-treated mice and thus calcium levels remain low and incretins are unable to stimulate release of endogenous insulin.

4.3 Glibenclamide – binding to the K_{ATP} channel leads to insulin secretion

Sulphonylurea drugs are specific K_{ATP} channel blockers [66]. Glibenclamide bypasses the metabolic stages and binds directly to K_{ATP} channels, which leads to membrane depolarization and insulin secretion. My studies suggest that maximal insulin secretion in induced iβ-V59M is triggered by 2μM glibenclamide. It is likely that a maximal drug concentration was achieved in mice implanted with glibenclamide pellets. Although I did not measure plasma glibenclamide concentrations in my mice, animals treated with 2.5mg/21 days (0.12mg/day) had glibenclamide concentrations of 0.75μM (males) and 1.5μM (females) (personal communication, Carolina Lahmann). My mice received 0.42mg/day (25mg/60days) and are thus likely to have had higher plasma drug levels.

4.3.1 The effect of glibenclamide on blood glucose and body weight

Glibenclamide (25mg/60 days) reversed the hyperglycaemia of induced iβ-V59M mice overnight and blood glucose levels remained very well controlled within a narrow range for 4 weeks (Figures 3.1). Even though glibenclamide concentrations were significantly higher than drug doses given to human patients, hypoglycaemia did not occur. Shimomura *et al* (unpublished) showed that full inhibition of K_{ATP} channels requires a higher glibenclamide dose than used in my experiment. Remedi *et al* (2009) reported that significantly lower glibenclamide concentrations (2.5mg/60 days) were unable to reverse hyperglycaemia when implanted in induced, hyperglycaemic mice expressing a gain-of-function K_{ATP} channel

mutation [89]. However, when implanted with the same glibenclamide pellet prior to gene induction, no increase in blood glucose levels was detected and they were maintained in a physiological range. Why the lower dose was effective when given before gene induction but not after diabetes onset is unclear. One possibility is that later-onset administration was unsuccessful at stimulating sufficient insulin release to maintain glucose homeostasis because of a hyperglycaemia-induced loss of beta-cell mass.

In a different set of experiments Remedi *et al* (2011) even achieved remission of diabetes with aggressive glibenclamide treatment before diabetes onset [99]. In a subset of mice treated in this way, the glibenclamide concentration then could be gradually reduced and eventually removed without elevation of blood glucose. However, this 'diabetes remission' only occurred in a small number of mice and the glibenclamide concentrations used were ~70 times higher than those used to treat human patients suffering from neonatal diabetes. Why this happens is unclear. One possibility is that β-cell mass recovers when glucose homestasis improves on glibenclamide therapy. If Cre recombinase is not activated in all β-cells (i.e. there is mosaic expression), so that some β-cells remain normal, there may be a sufficient recovery of normal β-cells to maintain glucose homeostasis. It might be interesting to investigate if a similar phenomenon is observed in our iβ-V59M mice. Some ND patients with specific mutations also show transient-remitting-diabetes, but the mechanism is unknown. However, this does not happen for patients with the Kir6.2-V59M mutation.

I had expected that blood glucose levels in wild-type mice would also be decreased with glibenclamide. However, glibenclamide treatment (2.5mg/21 days) led to a significant *increase* in blood sugar levels (Figure 3.21). Remedi and Nichols (2008) reported similar results and they argued that the loss of glucose tolerance is caused by β-cell desensitization and can be reversed by drug removal [100].

Glibenclamide therapy in induced iβ-V59M or wild-type mice had no effect on body weight (Figures 3.3), although it has been reported that type 2 diabetes mellitus patients gain body weight when treated with glibenclamide [83, 84] and neonatal diabetes patients seem to lose body weight. This suggests that metabolic effects in mice and humans may be different or that weight loss may have been observed if induced iβ-V59M mice were treated for longer than 4 weeks with glibenclamide.

4.3.2 Glibenclamide therapy fully preserves pancreatic islets

Visually, pancreatic islets stained for insulin after 4 weeks of glibenclamide therapy, were not obviously different from islets of control mice: Their shape was round, smooth and well-defined and the majority of the islet was occupied by insulin-positive cells (Figures 3.11). Also, glibenclamide fully preserved β-cell area, islet number, single islet size and total islet area (Figures 3.12).

Similarly, glibenclamide treatment preserved insulin content (Figures 3.10). Islets isolated from glibenclamide-treated mice responded significantly better to

tolbutamide than islets isolated from insulin- or placebo-treated mice, presumably because it fully preserved β-cell mass. Thus high-dose glibenclamide therapy maintains both the number and function of pancreatic β-cells. This indicates that it is not only essential to maintain blood glucose levels but also to ensure closure of the mutant K_{ATP} channels, in order to treat neonatal diabetes successfully. Our data also suggest that sulphonylurea drugs are actually better than insulin therapy for neonatal diabetes.

4.3.3 Glibenclamide partially, but no completely, corrects glucose tolerance

Glucose tolerance measured 2 and 4 weeks after glibenclamide pellet implantation was similar. The response to glucose was still impaired but significantly better than in placebo-treated induced iβ-V59M mice (Figures 3.6, 3.7). An incretin effect was seen in male treated iβ-V59M mice when glucose was given orally (Table 4). As K_{ATP} channel closure leads to an increase in intracellular Ca^{2+}, an incretin effect is expected.

4.4 Conclusion

This dissertation shows that severe and persistent hyperglycaemia plays a major role in the deterioration of pancreatic islets and β-cells. Treatment should be introduced as soon as hyperglycaemia is present. Insulin preserves blood glucose levels but does not affect the K_{ATP} channel and pancreatic islets and β-cells slowly decrease in number and lose their function. In contrast, sulphonylurea drugs,

which close β-cell K_{ATP} channels and stimulate endogenous insulin release, not only maintain physiological blood glucose levels but also preserve the morphology of the pancreatic islets and β-cells. These results suggest that it is not only important to maintain physiological blood glucose levels (~4mM) but also to close K_{ATP} channels in order to maintain the structure and function of the endocrine pancreas. These findings have implications for the therapy of human patients suffering from diabetes.

4.5 Future directions

As glucagon is the antagonist to insulin, and its release is impaired in type 2 diabetes, it would be interesting to examine how K_{ATP} channel overactivity affects α-cells and glucagon production. Preliminary data suggest that in mice expressing the Kir6.2-V59M mutation in pancreatic β-cells, glucagon-containing α-cells increase in number, and their distribution throughout the pancreatic islet changes. It might be interesting to investigate if the α-cell expansion is cause by β-cell death and subsequent α-cell proliferation or by transdifferentiation. This might be possible by immunohistochemical staining of cell proliferation markers (Ki-67 or PCNA). Pancreatic β-cells in our inducible iβ-V59M express GFP. If conversion of β-cells into α-cells occurs, then α-cells should express GFP and thus could be visualized with a GFP-specific antibody. The effect of expressing the Kir6.2-V59M mutation in pancreatic α-cells should also be examined.

References

1. Seino, S. and T. Miki, *Physiological and pathophysiological roles of ATP sensitive K+ channels.* Prog Biophys Mol Biol, 2003. 81(2): p. 133-76.
2. Yokoshiki, H., et al., *ATP-sensitive K^+ channels in pancreatic, cardiac, and vascular smooth muscle cells.* Am J Physiol Cell Physiol, 1998. 271(1): p. C25-37.
3. Cook, D.L. and C.N. Hales, *Intracellular ATP directly blocks K^+ channels in pancreatic B-cells.* Nature, 1984. 311(5983): p. 271-3.
4. Ashcroft, F.M., D.E. Harrison and S.J. Ashcroft, *Glucose induces closure of single potassium channels in isolated rat pancreatic beta-cells.* Nature, 1984. 312(5993): p. 446-8.
5. Rorsman, P. and G. Trube, *Glucose dependent K^+-channels in pancreatic β-cells are regulated by intracellular ATP.* Pflugers Arch, 1985. 405(4): p. 305-9.
6. Ashcroft, F.M., *The Walter B. Cannon Physiology in Perspective Lecture, 2007. ATP-sensitive K^+ channels and disease: from molecule to malady.* Am J Physiol Endocrinol Metab, 2007. 293(4): p. E880-889.
7. Hattersley, A.T. and F.M. Ashcroft, *Activating mutations in Kir6.2 and neonatal diabetes: new clinical syndromes, new scientific insights, and new therapy.* Diabetes, 2005. 54(9): p. 2503-13.
8. Pearson E.R., et al., *Switching from insulin to oral sulfonylureas in patients with diabetes due to Kir6.2 mutations.* N Engl J Med, 2006. 355(5): p. 467-77.
9. Shyng, S. and C.G. Nichols, *Octameric stoichiometry of the KATP channel complex.* J Gen Physiol, 1997. 110(6): p. 655-64.
10. Clement, J.P.4th., et al., *Association and stoichiometry of K(ATP) channel subunits.* Neuron, 1997. 18(5): p. 827-38.
11. Inagaki, N., et al., *Reconstitution of IKATP: an inward rectifier subunit plus the sulfonylurea receptor*. Science, 1995. 270(5239): p. 1166-70.
12. Inagaki, N., et al., *Cloning and functional characterization of a novel ATP-sensitive potassium channel ubiquitously expressed in rat tissues, including pancreatic islets, pituitary, skeletal muscle, and heart.* J Biol Chem, 1995. 270(11): p. 5691-4.
13. Sakura, H., et al., *Cloning and functional expression of the cDNA encoding a novel ATP-sensitive potassium channel subunit expressed in pancreatic beta-cells, brain, heart and skeletal muscle.* FEBS Lett, 1995. 377(3): p. 338-44.
14. Kan, L.Y. and Y.N. Jan, *Potassium channels and their evolving gates.* Nature, 1994. 371(6493): p. 119-22.
15. Akrouh A., et al., *Molecular Biology of K(ATP) channels and implications for health and disease.* IUBMB Life, 2009. 61(10): 971–8.
16. Tucker, S.J., et al., *Truncation of Kir6.2 produces ATP-sensitive K + channels in the absence of the sulphonylurea receptor.* Nature, 1997. 387(6629): p. 179-83.
17. Aguilar-Bryan, L., et al., *Cloning of the beta cell high-affinity sulfonylurea receptor: a regulator of insulin secretion.* Science, 1995. 268(5209): p. 423-6.
18. Ashcroft F.M., *K(ATP) channels and insulin secretion: a key role in health and disease.* Biochem Soc Trans, 2006. 34(2): 243-6.
19. Aittoniemi J., et al., Review. *SUR1: a unique ATP-binding cassette protein that functions as an ion channel regulator.* Phil Trans R Soc Lond B Biol Sci, 2009. 364(1514): 257–67.

20. Gribble, F.M., S.J. Tucker and F.M. Ashcroft, *The essential role of the Walker A motifs of SUR1 in K-ATP channel activation by Mg-ADP and diazoxide.* Embo J, 1997. 16(6): p. 1145-52.
21. Nichols, C.G., et al., *Adenosine diphosphate as an intracellular regulator of insulin secretion.* Science, 1996. 272(5269): p. 1785-7.
22. Mikhailov M.V., Mikhailova E.A. and Ashcroft S.J., *Molecular structure of the glibenclamide binding site of the beta-cell K(ATP) channel.* FEBS Lett, 2001. 499 (1-2): p. 154-60.
23. Ashcroft, F.M. and P. Rorsman, *Electrophysiology of the pancreatic beta-cell.* Prog Biophys Mol Biol, 1989. 54(2): p. 87-143.
24. Dunne, M.J. and O.H. Petersen, *Intracellular ADP activates K + channels that are inhibited by ATP in an insulin-secreting cell line.* FEBS Lett, 1986. 208(1): p. 59-62.
25. Kakei, M., et al., *The ATP-sensitivity of K + channels in rat pancreatic B-cells is modulated by ADP.* FEBS Lett, 1986. 208(1): p. 63-6.
26. Baukrowitz, T. and B. Fakler, *K(ATP) channels: linker between phospholipid metabolism and excitability.* Biochem Pharmacol, 2000. 60(6): p. 735-40.
27. Fan, Z. and J.C. Makielski, *Anionic phospholipids activate ATP-sensitive potassium channels.* J Biol Chem, 1997. 272(9): p. 5388-95.
28. Shyng, S.L. and C.G. Nichols, *Membrane phospholipid control of nucleotide sensitivity of KATP channels*. Science, 1998. 282(5391): p. 1138-41.
29. Kanno, T., P. Rorsman and S.O. Gopel, *Glucose-dependent regulation of rhythmicaction potential firing in pancreatic beta-cells by K(ATP)-channel modulation.* J Physiol, 2002. 545(Pt 2): p. 501-7.
30. Henquin J.C., *Triggering and amplifying pathways of regulation of insulin secretion by glucose.* Diabetes, 2000. 49(11): p. 1751-60.
31. Henquin J.C., *Regulation of insulin secretion: a matter of phase control and amplitude modulation.* Diabetologia, 2009. 52(2): p. 739-51.
32. Ahrén B., *Islet G protein-coupled receptors as potential targets for treatment of type 2 diabetes.*Nat Rev Drug Discov, 2009. 8(5): p. 369-85.
33. Parker H.E., F. Reimann and F.M Gribble, *Molecular mechanisms underlying nutrient-stimulated incretin secretion.* Expert Rev Mol Med, 2010. 12: e1.
34. Gloyn, A.L., et al., *Activating mutations in the gene encoding the ATP-sensitive potassium-channel subunit Kir6.2 and permanent neonatal diabetes.* N Engl J Med, 2004. 350(18): p. 1838-49.
35. Thomas, P., Y. Ye and E. Lightner, *Mutation of the pancreatic islet inward rectifier Kir6.2 also leads to familial persistent hyperinsulinemic hypoglycemia of infancy.* Hum Mol Genet, 1996. 5(11): p. 1809-12.
36. Thomas, P.M., et al., *Mutations in the sulfonylurea receptor gene in familial persistent hyperinsulinemic hypoglycemia of infancy.* Science, 1995. 268(5209): p. 426-9.
37. Dunne, M.J., et al., *Hyperinsulinism in infancy: from basic science to clinical disease.* Physiol Rev, 2004. 84(1): p. 239-75.
38. Gloyn, A.L., J. Siddiqui and S. Ellard, *Mutations in the genes encoding the pancreatic beta-cell KATP channel subunits Kir6.2 (KCNJ11) and SUR1 (ABCC8) in diabetes mellitus and hyperinsulinism.* Hum Mutat, 2006. 27(3): p. 220-31.
39. Glaser, B., et al., *Genetics of neonatal hyperinsulinism.* Arch Dis Child Fetal Neonatal Ed, 2000. 82(2): p. F79-86.
40. Nestorowicz, A., et al., *A nonsense mutation in the inward rectifier potassium channel gene, Kir6.2, is associated with familial hyperinsulinism.* Diabetes, 1997. 46(11): p.1743-8.

41. Lin, Y.W., et al., *A novel KCNJ11 mutation associated with congenital hyperinsulinism reduces the intrinsic open probability of beta-cell ATP-sensitive potassium channels.* J Biol Chem, 2006; 281:3006–3012.
42. Ashcroft, F.M., *ATP-sensitive potassium channelopathies: focus on insulin secretion.* J Clin Invest, 2005. 115(8): p. 2047-58.
43. Henwood, M.J., et al., *Genotype-phenotype correlations in children with congenital hyperinsulinism due to recessive mutations of the adenosine triphosphate-sensitive potassium channel genes.* J Clin Endocrinol Metab, 2005. 90(2): p. 789-94.
44. Marthinet, E., et al., *Severe congenital hyperinsulinism caused by a mutation in theKir6.2 subunit of the adenosine triphosphate-sensitive potassium channel impairing trafficking and function.* J Clin Endocrinol Metab, 2005. 90(9): p. 5401-6.
45. Polak, M. and J. Shield, *Neonatal and very-early-onset diabetes mellitus.* Semin Neonatol, 2004. 9(1): p. 59-65.
46. Flanagan, S.E., et al., *Mutations in ATP-sensitive K^+ channel genes cause transient neonatal diabetes and permanent diabetes in childhood or adulthood.* Diabetes, 2007. 56(7): p. 1930-7.
47. Girard, C.A., et al., *Functional analysis of six Kir6.2 (KCNJ11) mutations causing neonatal diabetes.* Pflugers Arch, 2006. 453(3): p. 323-32.
48. Edghill, E.L., et al., *Activating mutations in the KCNJ11 gene encoding the ATP-sensitive K + channel subunit Kir6.2 are rare in clinically defined type 1 diabetes diagnosed before 2 years.* Diabetes, 2004. 53(11): p. 2998-3001.
49. Sagen, J.V., et al., *Permanent neonatal diabetes due to mutations in KCNJ11 encoding Kir6.2: patient characteristics and initial response to sulfonylurea therapy.* Diabetes, 2004. 53(10): p. 2713-8.
50. Proks, P., et al., *Molecular basis of Kir6.2 mutations associated with neonatal diabetes or neonatal diabetes plus neurological features.* Proc Natl Acad Sci U S A, 2004. 101(50): p. 17539-44.
51. Proks, P., et al., *A gating mutation at the internal mouth of the Kir6.2 pore is associated with DEND syndrome.* EMBO Rep, 2005. 6(5): p. 470-5.
52. McTaggart J.S., R.H. Clark and F.M. Ashcroft, *The role of the KATP channel in glucose homeostasis in health and disease: more than meets the islet.* J Physiol, 2010. 588(17): p. 3201-9.
53. Flanagan S.E., et al., *Update of mutations in the genes encoding the pancreatic beta-cell K(ATP) channel subunits Kir6.2 (KCNJ11) and sulfonylurea receptor 1 (ABCC8) in diabetes mellitus and hyperinsulinism.* Hum Mutat, 2009. 30(2): p. 170-80.
54. Proks, P., et al., *A heterozygous activating mutation in the sulphonylurea receptor SUR1 (ABCC8) causes neonatal diabetes.* Hum Mol Genet, 2006. 15(11): p. 1793-800.
55. Proks, P., et al., *Mechanism of action of a sulphonylurea receptor SUR1 mutation (F132L) that causes DEND syndrome.* Hum Mol Genet, 2007. 16(16): p. 2011-9.
56. de Wet, H., et al., *A mutation (R826W) in nucleotide-binding domain 1 of ABCC8 reduces ATPase activity and causes transient neonatal diabetes.* EMBO Rep, 2008. 9(7): p. 648-54.
57. de Wet, H., et al., *Increased ATPase activity produced by mutations at arginine-1380 in nucleotide-binding domain 2 of ABCC8 causes neonatal diabetes.* Proc Natl Acad Sci U S A, 2007. 104(48): p. 18988-92.
58. Partridge, C.J., D.J. Beech and A. Sivaprasadarao, *Identification and pharmacological correction of a membrane trafficking defect associated with a mutation in the sulfonylurea receptor causing familial hyperinsulinism.* J Biol Chem, 2001. 276(38): p. 35947-52.

59. Henwood, M.J., et al., *Genotype-phenotype correlations in children with congenital hyperinsulinism due to recessive mutations of the adenosine triphosphate-sensitive potassium channel genes.* J Clin Endocrinol Metab, 2005. 90(2): p. 789-94.
60. Dacou-Voutetakis C., F. Psychou and M. Maniati-Christidis, *Persistent hyperinsulinemic hypoglycemia of infancy: long-term results.* J Pediatr Endocrinol Metab, 1998. 11 Suppl 1: p. 131-41.
61. Glaser B. and H. Landau, *Long-term treatment with the somatostatin analogue SMS 201-995: alternative to pancreatectomy in persistent hyperinsulinaemic hypoglycaemia of infancy.* Digestion, 1990. 45 Suppl 1: p. 27-35.
62. Glaser B., et al., *Persistent hyperinsulinaemic hypoglycaemia of infancy: long-term treatment with somatostatin analogue Sandostatin.* Clin Endocrinol (Oxf), 1989. 31(1): p. 71-80.
63. Bennett K., C. James and K. Hussain, *Pancreatic β-cell KATP channels: Hypoglycaemia and hyperglycaemia.* Rev Endocr Metab Disord, 2010. 11(3): p. 157-63.
64. Leibowitz G., et al., *Hyperinsulinemic hypoglycemia of infancy (nesidioblastosis) in clinical remission: high incidence of diabetes mellitus and persistent beta-cell dysfunction at long-term follow-up.* J Clin Endocrinol Metab, 1995. 80(2): p. 386-92.
65. Ashcroft F.M., *New uses for old drugs: neonatal diabetes and sulphonylureas.* Cell Metab, 2010. 11(3): p. 179-81.
66. Gribble, F.M. and F. Reimann, *Sulphonylurea action revisited: the post-cloning era.* Diabetologia, 2003. 46(7): p. 875-91.
67. Zung A., et al., *Glibenclamide treatment in permanent neonatal diabetes mellitus due to an activating mutation in Kir6.2.* J Clin Endrcrinol Metab, 2004. 89(11): p. 5504-7.
68. UK Prospective Diabetes Study (UKPDS) Group, *Intensive blood-glucose control with sulphonylureas or insulin compared with conventional treatment and risk of complications in patients with type 2 diabetes (UKPDS 33).* Lancet, 1998. 352(9131): p. 837-53.
69. The Diabetes Control and Complications Trial Research Group, *The effect of intensive treatment of diabetes on the development and progression of long-term complications in insulin-dependent diabetes mellitus.* N Engl J Med, 1993. 329(14): p. 977-86.
70. Slingerland, A.S., et al., *Improved motor development and good long-term glycaemic control with sulfonylurea treatment in a patient with the syndrome of intermediate developmental delay, early-onset generalized epilepsy and neonatal diabetes associated with the V59M mutation in the KCNJ11 gene.* Diabetologia, 2006. 49(11): p. 2559-63.
71. Mlynarski, W., et al., *Sulfonylurea improves CNS function in a case of intermediate DEND syndrome caused by a mutation in KCNJ11.* Nat Clin Pract Neurol, 2007. 3(11): p. 640-5.
72. Shimomura, K., et al., *A novel mutation causing DEND syndrome: a treatable channelopathy of pancreas and brain.* Neurology, 2007. 69(13): p. 1342-9.
73. Perley M.J. and D.M. Kipnis, *Plasma insulin responses to oral and intravenous glucose: studies in normal and diabetic subjects.* J Clin Invest, 1967. 46(12): p. 1954-62.
74. Elrickn H., et al., *Plasma insulin response to oral and intravenous glucose administration.* J Clin Endocrinol Metab, 1964. 24: p. 1076-82.
75. Creutzfeldt W., *The incretin concept today.* Diabetologia, 1979. 16(2): p. 75-85.

76. Orskoy C., A. Wettergren and J.J. Holst, *Biological effects and metabolic rates of glucagonlike peptide-17-36 amide and glucagonlike peptide-17-37 in healthy subjects are indistinguishable.* Diabetes, 1993. 42(5): p. 658-61.
77. Dupre J. et al., *Stimulation of insulin secretion by gastric inhibitory polypeptide in man.* J Clin Edocrinol Metab, 1973. 37(5): p. 826-8.
78. Drucker D.J., et al., *Glucagon-like peptide I stimulates insulin gene expression and increase cyclic AMP levels in a rat islet cell line.* Proc Natl Acad Sci U S A, 1987. 84(10): p. 3434-3438.
79. *McIntosh C.H., et al., Glucose-dependent insulinotropic polypeptide stimulation of lipolysis in differentiated 3T3-L1 cells: wortmannin-sensitive inhibition by insulin.* Endocrinology, 1999. 140(1): 398-404.
80. Nauck M., et al., *Reduced incretin effect in type 2 (non-insulin-dependent) diabetes.* Diabetologia, 1986. 29(1): p. 46-52.
81. Codner E., et al., *Sulphonylurea treatment in young children with neonatal diabetes: dealing with hyperglycaemia, hypoglycaemia, and sick days.* Diabetes Care, 2007. 30(5): p. e28-9.
82. Girard, C.A., et al., *Expression of an activating mutation in the gene encoding the KATP channel subunit Kir6.2 in mouse pancreatic beta cells recapitulates neonatal diabetes.* J Clin Invest, 2009. 119(1): p. 80-90.
83. Fischer S., et al., *Influence of treatment with acarbose or glibenclamide on insulin sensitivity in type 2 diabetic patients.* Diabetes Obes Metab, 2003. 5(1): p. 38-44.
84. Derosa G., et al., *Exenatide versus glibenclamide in patients with diabetes.* Diabetes Technol Ther, 2010. 12(3): p. 233-40.
85. Dor Y., et al., *Adult pancreatic beta-cells are formed by self-duplication rather than stem-cell differentiation.* Nature, 2004. 429(6987): p. 41-6.
86. The Jackson Laboratory: http://jaxmice.jax.org/strain/008122.html
87. Woods S.C. and R.J. Seeley, *Insulin as an adiposity signal*. Int J Obes Relat Metab Disord, 2001. 25 Suppl 5: p. S35-8.
88. Kim W. and J.M. Egan, *The role of incretins in glucose homeostasis and diabetes treatment.* Pharmacol Rev, 2008. 60(4): 470-512.
89. Remedi M.S., et al., *Secondary consequences of beta cell inexcitability: identification and prevention in a murine model of K(ATP)-induced neonatal diabetes mellitus. Cell Metab,* 2009. 9(2): p. 140-51.
90. Koster J.C., et al., *Targeted overactivity of beta cell K(ATP) channels induce profound neonatal diabetes.* Cell, 2000. 100(6): p. 645-54.
91. Marshak S., et al., *Impaired beta-cell functions induced by chronic exposure of cultured human pancreatic islets to high glucose.* Diabetes, 1999. 48(6): p. 1230-6.
92. Hoftiezer V. and A.M. Carpenter, *Comparison of streptozotocin and alloxan-induced diabetes in the rat, including volumetric quantitation of the pancreatic islets.* Diabetologia, 1973. 9(3): p. 178-84.
93. Li Z., F.A. Karlsson and S. Sandler, *Islet loss and alpha cell expansion in type 1 diabetes induced by multiple low-dose streptozotocin administration in mice.* J Endocrinol, 2000. 165(1): p. 93-9.
94. Takeda Y., et al., *Reduction of both beta cell death and alpha cell proliferation by dipeptidyl peptidase-4 inhibition in a streptozotocin-induced model of diabetes in mice.* Diabetologia, 2012. 55(2): p. 404-12.
95. Talchai C., et al., *Pancreatic β cell dedifferentiation as a mechanism of diabetic β cell failure.* Cell, 2012. 150(6): p. 1223-34.
96. Dor Y. and B. Glaser, *β-cell dedifferentiation and type 2 diabetes.* N Engl J Med, 2013. 368(6): p. 572-3.
97. Le May C., et al., *Estrogens protect pancreatic beta-cells from apoptosis and prevent insulin-deficient diabetes mellitus in mice.* Proc Natl Acad Sci USA, 2006. 103(24): p. 9232-7.

98. Aronoff S.L., et al., *Glucose metabolism and regulation: beyond insulin and glucagon.* Diabetes Spectrum, 2004. 17(3): p. 183-190.
99. Remedi M.S., et al., *Acute sulphonylurea therapy at disease onset can cause permanent remission on KATP-induced diabetes.* Diabetes, 2011. 60(10): p. 2515-22.
100. Remedi M.S. and C.G. Nichols, *Chronic antidiabetic sulphonylureas in vivo: reversible effects on mouse pancreatic beta-cells*. PLoS Med, 2008. 5(10): p. e206.